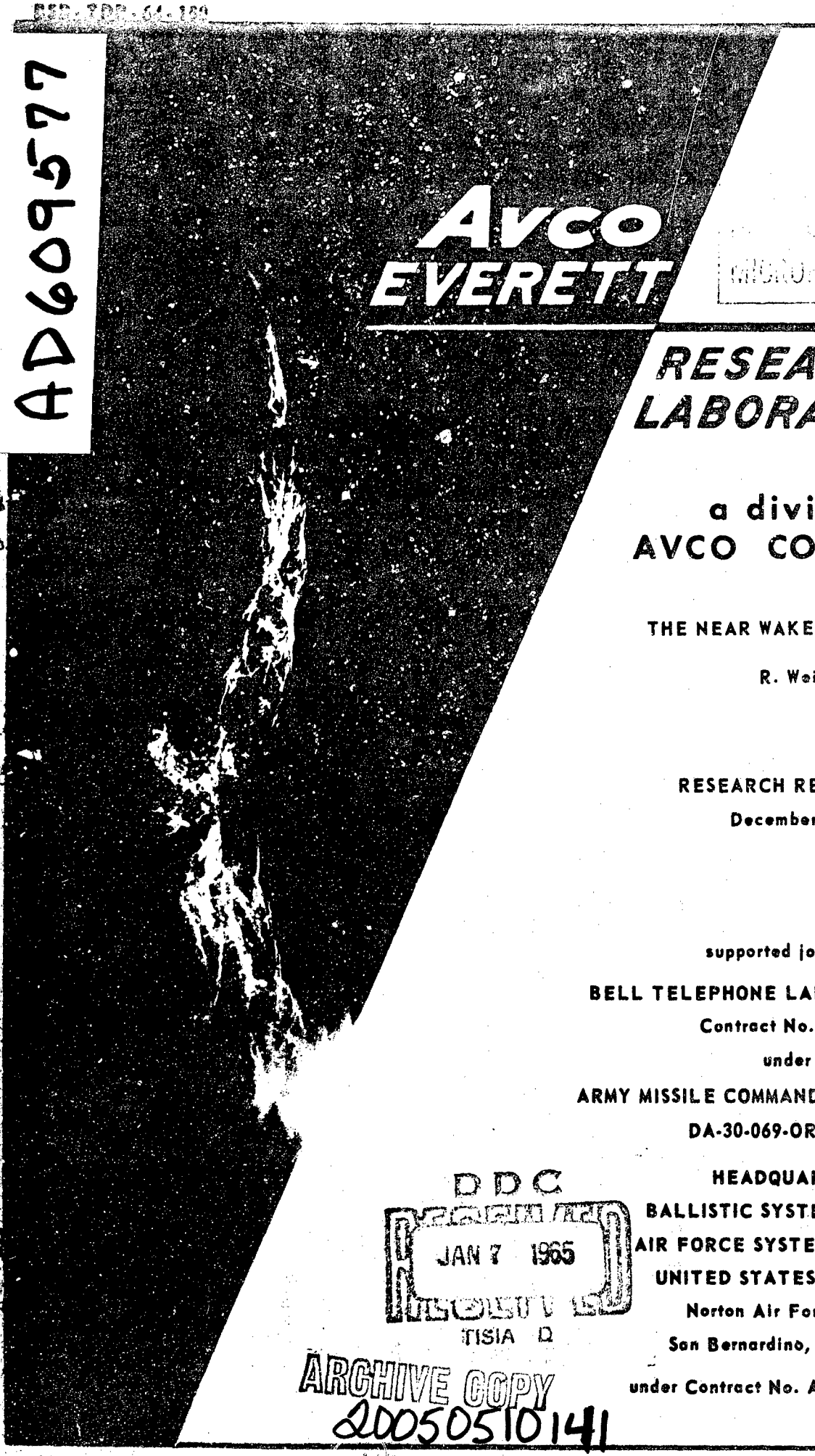

AVCO EVERETT RESEARCH LABORATORY

a division of
AVCO CORPORATION

THE NEAR WAKE OF A WEDGE

R. Weiss

RESEARCH REPORT 197
December 1964

supported jointly by
BELL TELEPHONE LABORATORIES, INC.
Contract No. 600767
under
ARMY MISSILE COMMAND PRIME CONTRACT
DA-30-069-ORD-1955

HEADQUARTERS
BALLISTIC SYSTEMS DIVISION
AIR FORCE SYSTEMS COMMAND
UNITED STATES AIR FORCE
Norton Air Force Base
San Bernardino, California
under Contract No. AF 04(694)-414

BSD-TDR-64-150

RESEARCH REPORT 197

THE NEAR WAKE OF A WEDGE

by

R. Weiss

AVCO-EVERETT RESEARCH LABORATORY
a division of
AVCO CORPORATION
Everett, Massachusetts

December 1964

supported jointly by

BELL TELEPHONE LABORATORIES, INC.
Contract No. 600767
under
ARMY MISSILE COMMAND PRIME CONTRACT
DA-30-069-ORD-1955

HEADQUARTERS
BALLISTIC SYSTEMS DIVISION
AIR FORCE SYSTEMS COMMAND
UNITED STATES AIR FORCE
Norton Air Force Base
San Bernardino, California

under Contract No. AF 04(694)-414

SYMBOLS

r, θ	polar coordinates
u, v	radial, tangential velocity components
P	pressure
ψ	streamfunction
R, β, α	see Fig. 1
μ, ν	absolute, kinematic viscosity
ρ	mass density
T	temperature
δ	boundary layer thickness; also, "variation of"
$[\ ]^{+}_{-}$	"jump" in quantity; "+" refers to free shear layer
M	Mach number
Re	Reynolds number
Pr	Prandtl number
Pe'	Péclet number
γ	ratio of specific heats
η	P_{t_D}/P_{neck}
h	static enthalpy
$\vec{V}$	velocity vector
C_p	specific heat
k	thermal conductivity
ω	vorticity
q	heat flux rate

Subscripts

r, θ	partial derivatives
1, 2, 3, 4,	flow field subregions (Fig. 1)
DSL	dividing-streamline quantity
D	dividing streamline quantity at matching point
t, o	stagnation condition
w	wall condition
*	dimensional quantity
H	inviscid flow conditions at $\nu = a$
B	recirculation region quantity
n	component normal to shock

Superscripts

'	ordinary derivative
1	first approximation
—	non-dimensional quantity

ABSTRACT

An analytical model of the two-dimensional laminar near wake is described. All relevant physical features of the flow, including the boundary layer expansion at the shoulder, free shear layers, recirculation regions and recompression region are included. A tractable problem is formulated by matching approximate solutions for each of these regions along mutual boundaries. A set of coupled algebraic equations is derived, and numerical results obtained for the conditions of a wind tunnel wedge experiment. Satisfactory agreement is obtained between the measured and theoretical variation of base pressure with Reynolds number. Additional computations are carried out for a series of wedges of different length, apex angle and wall temperature. The variation of base pressure, wake angle and neck enthalpy ratio with altitude is obtained for these bodies. It is shown that the near wake dimensions scale approximately with body size, and that the neck enthalpy ratio has a significant variation with body size, wall temperature and altitude. The effect of free-stream velocity on the neck enthalpy ratio is seen to be relatively unimportant, however. A number of extensions of the first-order model are suggested.

Introduction

The laminar near wake of a slender, sharp-edged hypersonic body is typical of a large class of unsolved problems in fluid mechanics known as separated flows. Typically a region of large pressure gradients, reversed flow, large variations in Mach number and non-adiabatic conditions, a separated flow probably requires the solution of the complete Navier-Stokes equations for its accurate description. For most boundary conditions, however, this problem becomes intractable. Analytic solutions of the near wake must therefore be based on simplified models, which then yield only approximate results. The importance of this problem[1] and the complexity of obtaining numerical solutions[2] nevertheless justify such an approach. The usefulness of a flow model is a function of both the physical content of its assumptions and its capacity for refinement. One such model, consisting of several subregions of the flow field matched along common boundaries, will be examined.

The flow field is represented in Fig. 1. It is described in terms of inviscid, boundary-layer (free shear layer) and recirculation regions. When the boundary layer thickness is very small compared to the base height, i.e., at high laminar Reynolds numbers, Chapman's original theory[3] as modified by Denison and Baum[4] should be adequate for two-dimensional flow. At the other limit, the wake of a flat plate or a needle, Goldstein's[5] and Viviand and Berger's[6] theories neglect the "Base Region" completely. The present analysis will attempt to deal with conditions for which the boundary layer is a significant fraction of the base height, and where coupling of the free shear layers and recirculation regions is important. Inclusion of the recirculation regions, therefore, constitutes the essential improvement on previous theories.

The "inviscid" regions are assumed to be described by the Prandtl-

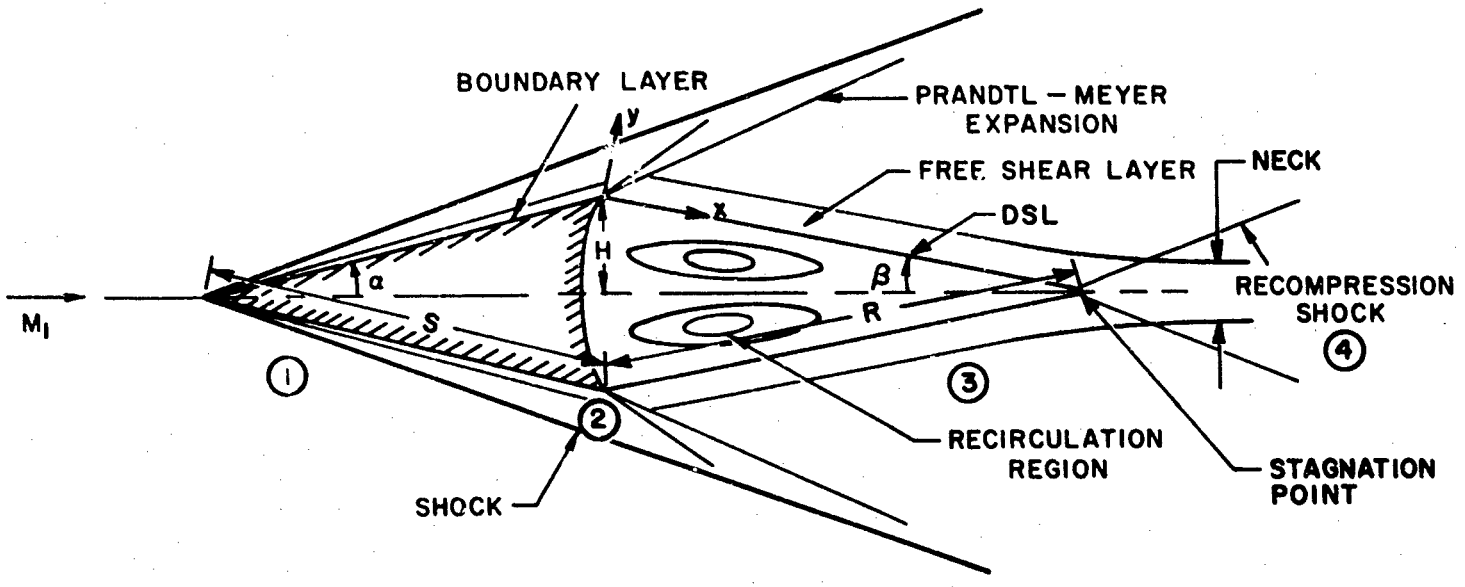

Fig. 1 The Near Wake Flow Field of a Wedge

Meyer relation, and the free shear layers (in general) by the Integral Boundary Layer Equations. The solution of the free shear layer with this method by Kubota and Dewey[7] suggests the approximation of a straight-line velocity profile between the dividing streamline and inviscid flow after a short transition distance from the shoulder. The relatively hot, low-density, low-velocity gas occupying the recirculation regions suggests that they can be approximately described with a streamfunction expansion in Reynolds number, the first term of which satisfies the biharmonic equation. An "elliptic" system which retains the highest order derivatives of the Navier-Stokes equations, the biharmonic equation is both physically and mathematically appropriate in these regions.* The influence of the boundary conditions in this region of reversed flow naturally results in the formulation of a boundary value problem, and the patching requirements along dividing streamlines demand retention of highest-order derivatives. This system allows for pressure gradients in all directions and can be solved independently of the energy equation. Most important of all, it is linear. While a streamfunction obtained from the biharmonic equation is a valid representation of a low Reynolds number, bounded flow field, an examination of the actual limitations of this approximation is given in the next section.

The requirements for matching the subregions are the continuity of pressure, velocity and shear. To make the problem tractable, some assumptions about the shape of the boundaries of each region are made. It is assumed that 1) the flow is symmetric about the center-line; 2) the dividing streamlines are straight and 3) the displacement thickness of the free shear layers is constant. Since the change in free shear layer thickness, δ_3, with distance is relatively small when the expanded boundary layer thickness, δ'_2, is a significant fraction of the base height, the assumption that $\delta_3 \cong \delta'_2$ is justified. Thus, we are assuming a constant pressure inviscid region (until the flow turns near the center-line) and cannot hope to match pressure at more than two points: at the base wall and at the important rear stagnation point. Furthermore, by avoiding the solution of the free shear layer we are restricted to matching of velocity and shear at one point on the

* M. Bloom has pointed out to the author that Ting and Bloom[8] first suggested this approach for cavity flows.

dividing streamline. The near wake geometry is then completely specified by the free shear layer thickness and the wake angle, β. The matching condition on the dividing streamline is thereby reduced to finding the magnitude of the dividing streamline velocity which is consistent with continuity of shear. Finally, the wake angle is determined by the continuity of pressure at the stagnation point of the dividing streamline, the well-known "Chapman recompression condition". Calculation of the stagnation pressure requires knowledge of the temperature field, and this is determined by an approximate solution of the energy equation. From this solution, it is possible to calculate the stagnation enthalpy of the dividing streamline as a function of all the flight parameters. Since the dividing streamline stagnation point is likely to be the hottest point in the flow field of a sharp, slender body, this calculation is of considerable practical importance.

I. Approximate Solution of the Recirculation Region

The "vorticity diffusion equation", the reduced form of the incompressible Navier-Stokes equations, is written in non-dimensional form as

$$\frac{1}{Re}\nabla^4\psi - \vec{V}\cdot\nabla(\nabla^2\psi) = 0 \qquad (1)$$

let us assume ψ to be an analytic function of Re and, therefore, an expansion of the form

$$\psi = \psi_o + Re\psi_1 + Re^2\psi_2 + \ldots .$$

which leads to a velocity field

$$\vec{V} = \vec{V}_o + Re\vec{V}_1 + \ldots .$$

The above expansion satisfies the equation of motion for arbitrary Re only if coefficients of all powers of Re vanish simultaneously: these conditions are

$$\nabla^4\psi_o = 0$$

$$\nabla^4\psi_1 = \vec{V}_o\cdot\nabla(\nabla^2\psi_o)$$

" "

etc. etc.

The expansion proposed is expected to be valid up to some Re_{max}, where an upper bound to Re_{max} is defined by

$$Re_{max} = \left(\frac{\psi_o}{\psi_1}\right)_{min} .$$

The first term in the expansion satisfies the biharmonic equation (the Stokes equations), and when substituted back into the full momentum equations, the first order pressure distribution may be calculated. For example, along the dividing streamline in a Cartesian coordinate system constructed as shown in Fig. 1,

$$P_{x_o} = \frac{1}{Re}\nabla^2 u_o - u_o u_{x_o}$$

and the important inertia terms appear. In fact, available experimental evidence,[17] together with the solution that will be obtained here (Fig. 3), indicate that

$$\frac{1}{Re}\nabla^2 u_o \ll u_o u_{x_o}$$

over most of the recompression portion of the dividing streamline (velocity profile inflection point is at $\psi = 0$) for $u_D R/\nu_w > 10$. During recompression, then,

$$P_{x_o}\Big|_{DSL} \approx u_o u_{x_o}\Big|_{DSL} \quad \text{or} \quad P_{t_o} \approx \text{constant.}$$

The assumption of a constant total pressure recompression process will therefore be made. It is, of course, possible to carry out the integration to obtain

$$P_{stag_o} - P_{base_o} = \int_o^R \left[\frac{1}{Re}\nabla^2 u_o - u_o u_{x_o}\right]_{DSL} dx$$

and obtain a higher stagnation pressure. This effect is obviously Reynolds number-dependent.

It is important to note that the usual test of the validity of the "Stokes Streamfunction", namely that the ratio of inertia terms to viscous terms be required to be less than unity, has not been used. Weinbaum[9]

has pointed out that this commonly used criterion is too severe. Wherever this test leads to ratios less than unity, however, the expansion used above will be valid. Since the calculation is simple, we will compute this ratio in the radial and tangential momentum equations:

$$S_o^{(r)} = \frac{1}{\nu}\left(\frac{ruu_r + vu_\theta - v^2}{ru_{rr} + u_r - \frac{1}{r}u + \frac{1}{r}u_{\theta\theta} - \frac{2}{r}v_\theta}\right)_o$$

$$S_o^{(\theta)} = \frac{1}{\nu}\left[\frac{uv_r + \frac{v}{r}v_\theta + \frac{uv}{r}}{v_{rr} + \frac{1}{r}v_r - \frac{v}{r^2} + \frac{1}{r^2}v_{\theta\theta} + \frac{2}{r^2}u_\theta}\right]_o$$

These may be written (with $\bar{r} = r/R$, $\bar{u} = u/u_D$)

$$\frac{S_o^{(\bar{r})}}{Re} = G_1(\bar{r}, \theta, \beta)$$

$$\frac{S_o^{(\theta)}}{Re} = G_2(\bar{r}, \theta, \beta)$$

The equations of motion are written in polar coordinates whose origin is at the stagnation point (Fig. 1), the resulting concavity in the base wall being insignficant for small wake angles. The streamfunction is then defined by

$$\left.\begin{aligned} u &= -\frac{1}{r}\psi_\theta \\ v &= \psi_r \end{aligned}\right\} \qquad (2)$$

The first term in the expansion in Re, ψ_o, must therefore satisfy

$$\nabla^4\psi_o = \left[\psi_{rrrr} + \frac{2}{r}\psi_{rrr} - \frac{1}{r^2}\psi_{rr} + \frac{1}{r^3}\psi_r + \frac{1}{r^4}\psi_{\theta\theta\theta\theta} + \frac{2}{r^2}\psi_{\theta\theta rr} - \frac{2}{r^3}\psi_{\theta\theta r} + \frac{4}{r^4}\psi_{\theta\theta}\right]_o = 0 \qquad (3)$$

The boundary conditions are:

$$\left.\begin{array}{lll} \text{(i)} & \text{at } r = 0: & u = 0 = v \\ \text{(ii)} & \text{on } r = R: & u = 0 = v \\ \text{(iii)} & \text{on } \theta = \pm\beta: & u = u_{DSL}(r);\ v = 0 \end{array}\right\} \tag{4}$$

Note that $u_{DSL}(r)$ must be determined from the matching conditions, and the boundary conditions reduce to:

$$\left.\begin{array}{lll} \text{(i)} & \text{at } r = 0: & \frac{1}{r}\psi_\theta = 0 = \psi_r \\ \text{(ii)} & \text{on } r = R: & \psi_\theta = 0 = \psi_r \\ \text{(iii)} & \text{on } \theta = \pm\beta: & -\frac{1}{r}\psi_\theta = u_{DSL}(r);\ \psi_r = 0 \end{array}\right\} \tag{5}$$

It is known that the solution to such a Boundary Value Problem exists and is unique.[10] It is further known that the solution satisfies (in addition to the Boundary Conditions) the Variational Principle:

$$\int_{-\beta}^{\beta}\int_{o}^{R} \nabla^4\psi_o \delta\psi_o r dr d\theta = 0 \tag{6}$$

The Ritz Method may be used to obtain an approximate solution for $\psi_o(r,\theta)$. Expanding ψ_o in a set of suitable functions which satisfy the Boundary Conditions:

$$\psi_o = \sum_{m=1}^{\infty} a_m g_m(r) f_m(\theta) \tag{7}$$

If both g_m and f_m are assumed, based on the expected behavior of the solution, substitution into Eq. (6) will result in an infinite set of algebraic equations for the a_m. A more accurate procedure is to assume only the $g_m(r)$-functions, and solve ordinary differential equations for $f_m(\theta)$ (which include the a_m). Accurate representation of the velocity profile will be important in the matching procedure, and this latter approach entails little difficulty. Substituting Eq. (7) into (6), and noting that δf_m is arbitrary, yields:

$$\sum_{m=1}^{\infty}\int_{o}^{R} r g_p \nabla^4(g_m f_m) dr = 0 \tag{8}$$

$$\text{for } p = 1, 2, 3, \ldots .$$

an infinite set of coupled, ordinary differential equations with constant coefficients. The general solutions are

$$f_m = c_{m1}f_{m1} + c_{m2}f_{m2} + c_{m3}f_{m3} + c_{m4}f_{m4} \tag{9}$$

with the c_m's determined by the remaining boundary conditions on $\theta = \pm \beta$. If the g_m's are chosen to be an orthonormal set,* important simplifications are possible. In addition, we may then expand $-ru_{DSL}(r)$ in such a set and obtain:

$$\left.\begin{aligned} -ru_{DSL}(r) &= \sum_{m=1}^{\infty} b_m g_m \\ \text{where } b_m &= -\int_o^R r^2 u_{DSL}(r) g_m dr \end{aligned}\right\} \tag{10}$$

(If non-orthogonal functions are used, Eqs. (8) are coupled; in addition, the b_m must be determined by another procedure).

The symmetry of the flow may now be used to eliminate the even functions in f_m (since ψ must be odd; i.e., anti-symmetrical) and obtain

$$f_m = c_{m1}f_{m1} + c_{m2}f_{m2} \tag{11}$$

The conditions [(5)-(iii)] may be written:

$$\left.\begin{aligned} \sum_{m=1}^{\infty} g_m f_m'(\beta) &= \sum_{m=1}^{\infty} b_m g_m \\ \sum_{m=1}^{\infty} g_m f_m(\beta) &= 0 \end{aligned}\right\} \tag{12}$$

Substituting Eq. (11) into (12) yields

$$\left.\begin{aligned} c_{m1}f_{m1}'(\beta) + c_{m2}f_{m2}'(\beta) &= b_m \\ c_{m1}f_{m1}(\beta) + c_{m2}f_{m2}(\beta) &= 0 \\ \text{for } m &= 1, 2, 3, \ldots . \end{aligned}\right\} \tag{13}$$

---

*calculated for various geometries by Chandrasekhar;[11] "completeness" has not been proved for this or any other applicable set.

This system must be truncated at some m = M, giving a total of 2M equations for 2M constants. But $u_{DSL}(r)$ can then be matched at only M points to determine the M values of b_m. It should be noted here that no proof can be given for completeness of the g_m set, and the convergence of ψ as $M \to \infty$ can only be shown by "numerical experiment".

For these boundary conditions, orthonormal functions have the disadvantage of being difficult to integrate, and it is helpful to choose another "relatively complete set" suggested by Kantorovich,[12]

$$g_m = r^{m+2}\left(1 - \frac{r}{R}\right)^2 \tag{14}$$

In addition to satisfying the boundary conditions [(5)-(i) and (5)-(ii)], these functions have the property that Eqs. (1) are bounded as $r \to 0$.

Choosing m = p = M = 1 in Eq. (8) yields an equation for f_1:

$$f_1'''' + 15.33 f_1'' + 75.66 f_1 = 0 \tag{15}$$

In this first-order approximation, we obtain

$$u_{DSL} = -r^2\left[1 - \frac{r}{R}\right]^2 f_1'(\beta) \tag{16}$$

Defining

$$u_D = u_{DSL_{max}} \tag{17}$$

we calculate from Eq. (16)

$$f_1'(\beta) = -\frac{16}{R^2}\, u_D$$

and

$$u_{DSL} = 16\left(\frac{r}{R}\right)^2\left[1 - \frac{r}{R}\right]^2 u_D \tag{18}$$

The conditions to be satisfied by Eq. (15) are then

$$\left.\begin{aligned} f_1(\beta) &= 0 \\ f_1'(\beta) &= -\frac{16 u_D}{R^2} \end{aligned}\right\} \tag{19}$$

and the solution is

$$\psi_{o_1}(\bar{r},\theta) = \frac{16u_D R}{\Gamma}\bar{r}^3(1-\bar{r})^2(z\sinh a\theta\cos b\theta - \cosh a\theta\sin b\theta)$$

where $\Gamma = b\cosh a\beta\cos b\beta + a\sinh a\beta\sin b\beta - z\,(a\cosh a\beta\cos b\beta - b\sinh a\beta\sin b\beta)$

and $z = \dfrac{\tan b\beta}{\tanh a\beta}$; $a = .74$, $b = 2.86$ (20)

$S_o^{(\bar{r})}/Re$ and $S_o^{(\theta)}/Re$ may now be evaluated for representative wake geometries. In particular, calculations carried out at 121 mesh points for $\beta = .10, .15, .20, .30, .40$ and $.50$ radians yield the following results:

a) the variation of $S_o^{(\bar{r})}/Re$ and $S_o^{(\theta)}/Re$ with β is small

b) $\dfrac{S_o^{(\theta)}}{Re} \sim 10^{-2}\ \dfrac{S_o^{(\bar{r})}}{Re}$ in general

c) $S_o^{(\bar{r})}/Re$ varies many orders of magnitude over the recirculation region, but a "histogram" display indicates the overwhelming (80%) frequency of

$$\frac{S_o^{(\bar{r})}}{Re} \sim \mathcal{O}(5 \times 10^{-3})$$

Thus, this severe test results in ψ_o being a good representation of ψ over 80% of the region for $Re = \rho_3 u_D R/\mu_W$ up to 200. Since it can be shown that typical values of Re are of this size, the expansion is valid over most of the region. Finally, since ψ_o satisfies the boundary conditions exactly, ψ_o is an exact solution on the dividing streamline, precisely where the more severe comparison of various derivatives of ψ would indicate ψ_o to be a poor representation of ψ_{exact}. Thus, ψ_o should be a satisfactory engineering estimate of ψ for the low Re cases under consideration. Furthermore, two additional refinements can be made:

A. Calculation of ψ_1

Using the variational principle[12]

$$\delta\iint\left\{(\nabla^2\psi_1)^2 - 2\psi_1\vec{V}_o\cdot\nabla(\nabla^2\psi_o)\right\}\bar{r}d\bar{r}d\theta = 0$$

we can expand ψ_1 as

$$\psi_1 = \sum_{m=1}^{\infty} f_{m1}(\theta) g_{m1}(\bar{r})$$

and proceed as before for ψ_o, imposing homogeneous boundary conditions on f_{m1} and g_{m1}.

B. Approximation of the Inertia Terms with a Modified Oseen Technique:

Since the high Reynolds number recirculation region has been shown by Batchelor[23] to consist of an "inviscid core" surrounded by boundary layers, it is necessary to accurately approximate the inertia terms only in these thin regions. The "modified Oseen technique" replaces the convective velocity there by a given suitable average velocity and thereby linearizes the Navier-Stokes equations. Weinbaum[18] has shown (in a cylindrical geometry) that this approximation leads to a smooth transition to the "Stokes" solution with decreasing Reynolds number.

II. Free Shear Layer Approximation and Matching Conditions

On the DSL, for m = p = M = 1, the matching is carried out at one point, chosen to be r = R/2 (where $u_{DSL} = u_D$). Thus it is prescribed that

$$\begin{aligned} &\text{(i)} && \left[u_{DSL}\right]_-^+ = 0 && \text{at } r = R/2 \\ &\text{(ii)} && \left[\tau_{DSL}\right]_-^+ = 0 && \text{at } r = R/2 \\ &\text{(iii)} && \left[P_{DSL}\right]_-^+ = 0 && \text{at } r = R/2 \end{aligned} \qquad (21)$$

Assuming $u_{DSL}{}^+ = 16\left(\frac{r}{R}\right)^2\left[1-\frac{r}{R}\right]^2 u_D{}^+$, we require that $u_D{}^+ = u_D{}^-$.

The pressure continuity can only be satisfied approximately since the dividing streamline shape is given, and only (i) and (ii) will be satisfied here. Then u_D is determined by [(21)-(ii)];

$$\tau_D^+ = \tau_D^- \tag{22}$$

Using the observation made before concerning free shear layer solutions, it is assumed that the velocity profile between DSL and edge of the free shear layer is linear and the shear is given by

$$\tau_D^+ = \frac{\mu_D}{\delta_3}\left[u_3 - u_D\right] \tag{23}$$

From Eq. (20) we may compute τ_D^-:

$$\tau_D^- = \frac{4ab}{\Gamma R}\,\mu_D u_D\,[z \cosh a\beta \sin b\beta + \sinh a\beta \cos b\beta] \tag{24}$$

From Eq. (22) and Fig. 1,

$$\frac{u_D}{u_3} = \frac{1}{1 + N\left(\frac{\delta_3}{\delta_2}\right)\left(\frac{\delta_2}{S}\right)\left(\frac{\sin\beta}{\sin\alpha}\right)} \tag{25}$$

where

$$N = \frac{4ab}{\Gamma}\,[z \cosh a\beta \sin b\beta + \sinh a\beta \cos b\beta].$$

We will assume δ_3 to be the thickness of the expanded boundary layer at the shoulder, thus neglecting the shear layer calculations. This approximation is certainly valid for thick shoulder boundary layer thicknesses, and the important interaction is the effect of u_D on τ_D.

III. Shoulder Expansion

Since an exact solution of the corner expansion of a supersonic boundary layer is not available, the relatively simple streamtube method will be employed to estimate δ_2'/δ_2. Assuming an isentropic expansion of each streamtube to pressure P_2 (determined by turning the inviscid flow through an angle $\nu = \alpha + \beta$), and conserving mass in streamtubes, it is possible to calculate the velocities and streamline locations after expansion (details of this calculation are given in Appendix I). Specific results are obtained with the good approximation for hypersonic boundary layers of a linear velocity profile and Busemann Integral enthalpy profile. The boundary

layer thickness before expansion is taken from Truitt[13] for insulated walls, and it is seen in Schlichting[14] (for representative Mach numbers) that cold wall thicknesses are well within a factor of two of the adiabatic results.

IV. Recompression Process

The final matching condition consists of equating the dividing streamline pressure at the stagnation point to the local value of the inviscid pressure field. Since the inviscid flow is not, in general, horizontal at this location, the pressure is less than the neck pressure. Assuming isentropic processes exterior to the free shear layer,

$$P_{neck} \approx P_3(\nu = \alpha) \equiv P_H \tag{26}$$

Then, $P_{stag} = \eta P_H$, where η depends on the "re-attachment" process in the neck. A typical value calculated by Reeves[15] gives $\eta \approx .6$. It is now assumed that the total pressure on the dividing streamline is approximately constant during recompression, and is therefore equal to P_t at the matching point ($\bar{r} = 1/2$). This assumption, discussed in a previous section, physically consists of a division of the dividing streamline into two parts: a region of acceleration by shear forces, in which the free shear layer does work to increase the kinetic energy of the DSL, and a region of isentropic recompression, in which further pressure rise due to shear forces is relatively insignificant.

We may therefore write

$$P_3 \left[1 + \frac{\gamma - 1}{2} M_3^2 \left(\frac{u_D}{u_3} \right)^2 \left(\frac{T_3}{T_D} \right) \right]^{\gamma/\gamma-1} = \eta P_H \,. \tag{27}$$

It is to be noted that η is dependent on the length of the recompression region in the free shear layer, and can be expected to decrease as Reynolds number decreases.

V. Solution of the Energy Equation in the Recirculation Region

Consistent with approximations made in the solution of the momentum equations, we will assume the density to be approximately constant in the low Mach number recirculation region. We may then neglect friction and

compression work in the energy equation[16] and write:

$$P\acute{e}\vec{V}\cdot\nabla h = \nabla^2 h \tag{28}$$

where

$$\vec{V} = \vec{i}u + \vec{j}v$$

$$u = u_*/u_D, \quad v = v_*/u_D, \quad \bar{r} = r/R$$

$$h = h_*/h_D \text{ and } P\acute{e} = PrRe = \left(\frac{C_p\mu}{k}\right)\left(\frac{u_D R}{\nu}\right)$$

The boundary conditions are:

$$\begin{aligned} &\text{(i)} && h = f(\bar{r}) && \text{on } \theta = \beta \\ &\text{(ii)} && \frac{\partial h}{\partial \theta} = 0 && \text{on } \theta = 0 \\ &\text{(iii)} && h = f(1) && \text{on } \bar{r} = 1 \end{aligned} \tag{29}$$

where $f(\bar{r})$ is to be specified. To obtain homogeneous boundary conditions, set

$$h = f(\bar{r}) + \bar{h}(\bar{r}, \theta) \tag{30}$$

and obtain

$$-P\acute{e}\left[u\frac{\partial \bar{h}}{\partial \bar{r}} + \frac{v}{\bar{r}}\frac{\partial \bar{h}}{\partial \theta}\right] + \nabla^2\bar{h} = G(P\acute{e}, \bar{r}, \theta) \tag{31}$$

where $G = +P\acute{e}\, u f' - \frac{f'}{\bar{r}} - f''$ is a known function.

The resulting nonhomogeneous equation is linear, since $\vec{V}$ has been obtained. An expansion of $\bar{h}$ in $P\acute{e}$-number is the simplest approach to a solution, but cannot be expected to converge for Reynolds numbers as high as those found valid for the momentum equation. This is because isotherms are generally expected to be non-parallel to streamlines due to the wall and axis boundary conditions, and $P\acute{e}\vec{V}\cdot\nabla h$ is non-negligible for flight $P\acute{e}$-numbers (the equivalent term in the vorticity diffusion equation was $Re\cdot\vec{V}\cdot\nabla\omega$, which can be small due to the nearer coincidence of vorticity contours and streamlines[9]). We must therefore retain the convective terms and deal with the variable coefficients in some approximate manner. The procedure adopted is to solve the equivalent "Galerkin" formulation of the problem (see Kantorovich[12]).

Let

$$\bar{h} = \sum_{j=1}^{\infty} \sum_{k=1}^{\infty} a_{jk} \chi_j(\bar{r}) g_k(\theta) \tag{32}$$

with the $\chi_k(\bar{r})$ taken to be a complete set of functions satisfying the boundary conditions:

$$\begin{aligned} &\text{(i)} \quad \bar{h}(0, \theta) = 0 \\ &\text{(ii)} \quad \bar{h}(1, \theta) = 0 \end{aligned} \tag{33}$$

The functions $\chi_j = \sin j\pi\bar{r}$ are therefore suitable. The boundary conditions

$$\begin{aligned} &\text{(iii)} \quad \bar{h}(\bar{r}, \beta) = 0 \\ &\text{(iv)} \quad \frac{\partial \bar{h}}{\partial \theta}(\bar{r}, 0) = 0 \end{aligned} \tag{34}$$

are satisfied by even functions comprising a "relatively complete" set:[12]

$$g_k(\theta) = (1 - \theta^2/\beta^2)\theta^{2(k-1)} \tag{35}$$

Thus, the N/M approximation is given by

$$\bar{h}_M^{(N)} = (1 - \theta^2/\beta^2) \sum_{j=1}^{M} \sum_{k=1}^{N} a_{jk} \theta^{2(k-1)} \sin j\pi\bar{r} \tag{36}$$

The solution (the a_{jk}'s) will be determined from the equivalent Galerkin formulation:

$$\int_0^{\beta} \int_0^{1} \left[L(\bar{h}_M^{(N)}) - G \right] \chi_j g_k \bar{r} d\bar{r} d\theta = 0 \tag{37}$$

for $j = 1, 2, \ldots M$

$k = 1, 2, 3, \ldots N$

with

$$L \equiv \nabla^2 - Pe\left[u \frac{\partial}{\partial \bar{r}} + \frac{v}{\bar{r}} \frac{\partial}{\partial \theta} \right]$$

$$\left.\begin{aligned} u^{(o)} &= 16\bar{r}^2(1 - \bar{r})^2 \frac{F'(\theta)}{\Gamma} \\ v^{(o)} &= -16r^2(1 - \bar{r})(3 - 5\bar{r}) \frac{F(\theta)}{\Gamma} \end{aligned}\right\} \text{ from Eqs. (2) and (20) with } \vec{u} \parallel \vec{r}$$

$$F(\theta) = z \sinh a\theta \cos b\theta - \cosh a\theta \sin b\theta$$

and

$$P\acute{e} \equiv \left(\frac{\rho_B u_3 S}{\mu_w}\right)\left(\frac{\sin a}{\sin \beta}\right)\frac{u_D}{u_3}\,Pr$$

We have assumed the Prandtl number to be constant and ρ_B to be approximately P_3/RT_W in this first iteration. To simplify the integration here, and to provide polynomial coefficients for a possible series solution, $F(\theta)$ and $F'(\theta)$ will be approximated as follows:

$$F(\theta) \cong m\theta(1 - \theta/\beta) \tag{38}$$

$$F'(\theta) \cong \Gamma\left\{\left[\frac{1-(\theta/\beta)^2}{1-(\theta_o/\beta)^2}\right] - 1\right\} = \Gamma\left\{a_o(1 - \theta^2/\beta^2) - 1\right\} \tag{39}$$

It is seen in Figs. (2) and (3) that $F'(\theta)$ is very well represented with $\theta_o/\beta \approx .55$ over a large range of β. The approximation of $F(\theta)$ should be most accurate near $\theta = \beta$, and can be poorly represented near $\theta = 0$, where $\partial h/\partial\theta \to 0$. Thus, m is required to minimize the average weighted error in the interval (o, β):

$$\int_o^\beta \theta\left[m\theta(1 - \theta/\beta) - F(\theta)\right] d\theta = 0 \tag{40}$$

a typical solution is given in Fig. (4), and m is given in Appendix II.

We expect that thermal boundary layers will form at even moderate Pé-numbers, and the approximate solution must reflect this behavior. Convection is expected to decrease temperatures on the dividing streamlines and increase them on the axis, indicating that a reasonable approximation may be obtained with M = 1 and N = 2. Proceeding from Eq. (36)

$$\bar{h}_1^{(2)} = (1 - \theta^2/\beta^2)\left[a_{11} + a_{12}\theta^2\right]\sin\pi\bar{r} \tag{41}$$

and we must solve the equations:

$$\left.\begin{aligned}
&\int_o^\beta\int_o^1 \left[L(\bar{h}_1^{(2)}) - G\right](1 - \theta^2/\beta^2)\sin\pi\bar{r}\bar{r}d\bar{r}d\theta = 0 \\
&\int_o^\beta\int_o^1 \left[L(\bar{h}_1^{(2)}) - G\right](1 - \theta^2/\beta^2)\theta^2\sin\pi\bar{r}\bar{r}d\bar{r}d\theta = 0
\end{aligned}\right\} \tag{42}$$

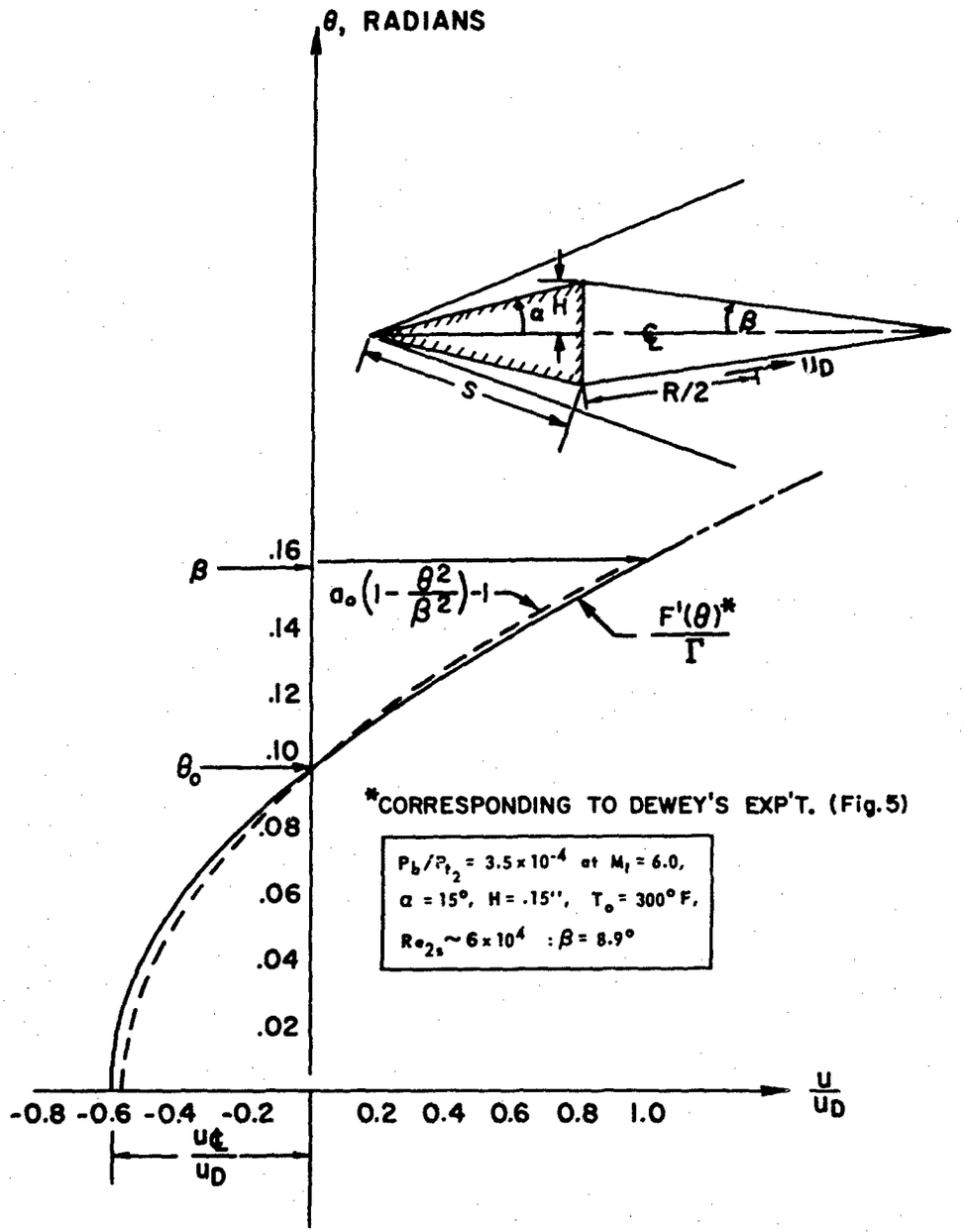

Fig. 2 Approximation for $\frac{F'(\theta)}{\Gamma}$ for $\beta = .16$ radians;

where $\left.\frac{u^{(o)}}{u_D}\right|_{\bar{r}=.5} = \frac{F'(\theta)}{\Gamma}$

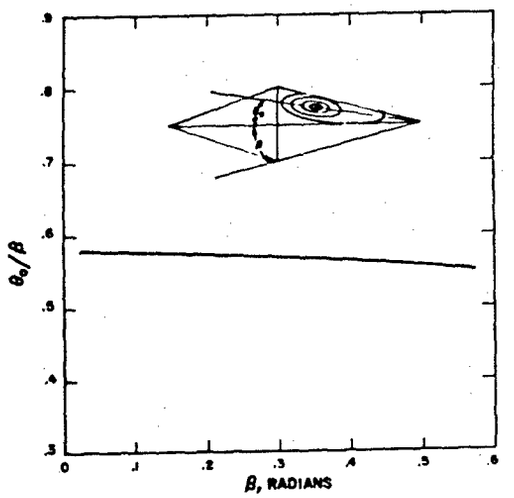

Fig. 3 Core location, θ_o/β, vs β

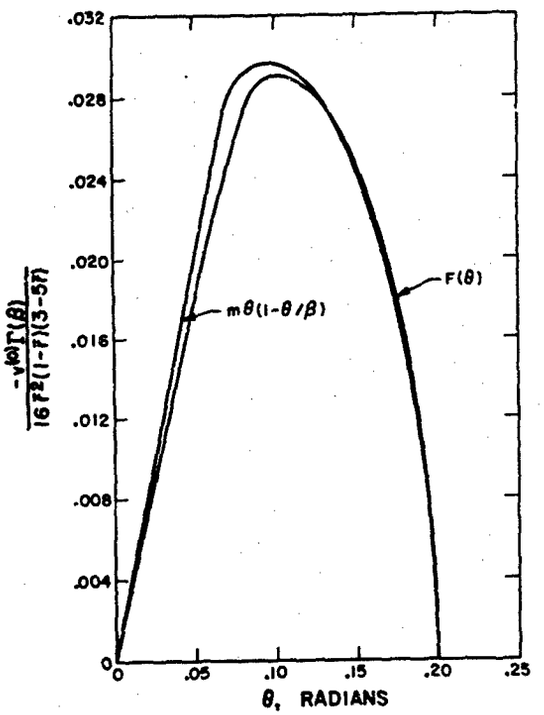

Fig. 4 Approximation for $F(\theta)$ for $\beta = 0.2$ radians; where $v^{(o)} = -16\bar{r}^2(1-\bar{r})^2 F(\theta)/\Gamma$

A2632
A2633

where $L(\bar{h}_1^{(2)}) =$

$$\frac{\partial^2 \bar{h}_1^{(2)}}{\partial \bar{r}^2} + \frac{1}{\bar{r}} \frac{\partial \bar{h}_1^{(2)}}{\partial \bar{r}} + \frac{1}{\bar{r}^2} \frac{\partial^2 \bar{h}_1^{(2)}}{\partial \theta^2} - P\acute{e}\left[u^{(o)} \frac{\partial \bar{h}_1^{(2)}}{\partial \bar{r}} + \frac{v^{(o)}}{\bar{r}} \frac{\partial \bar{h}_1^{(2)}}{\partial \theta}\right]$$

$$= -(1 - \theta^2/\beta^2)\left[a_{11}\pi^2 \sin\pi\bar{r} + a_{12}\theta^2\pi^2 \sin\pi\bar{r}\right]$$

$$+ \frac{1}{\bar{r}}(1 - \theta^2/\beta^2)\left[a_{11}\pi\cos\pi\bar{r} + \pi a_{12}\theta^2\cos\pi\bar{r}\right] \qquad (43)$$

$$+ \frac{1}{\bar{r}^2}\left[-\frac{2a_{11}}{\beta^2}\sin\pi\bar{r} + a_{12}\sin\pi\bar{r}\left(2 - \frac{12\theta^2}{\beta^2}\right)\right]$$

$$- P\acute{e}\left\{16\bar{r}^2(1-\bar{r})^2\left[a_o(1 - \theta^2/\beta^2) - 1\right]\left[1 - \theta^2/\beta^2\right]\left[a_{11}\pi\cos\pi\bar{r} + \pi a_{12}\theta^2\cos\pi\bar{r}\right]\right.$$

$$\left. - 16\frac{\bar{r}^2}{\bar{r}}(1-\bar{r})(3-5\bar{r})\frac{m}{\Gamma}\theta(1-\theta/\beta)\left[-\frac{2\theta a_{11}}{\beta^2}\sin\pi\bar{r} + 2\theta a_{12}\sin\pi\bar{r}\left(1-2\theta^2/\beta^2\right)\right]\right\}$$

To proceed further, we must specify $f(\bar{r})$. This is done by assuming a linear change from h_w to h_D, followed by a constant total enthalpy recompression. These assumptions are consistent with those employed in solution of the momentum equations ($P_t(o, \beta) \approx P_t(1/2, \beta)$):

$$f(\bar{r}) = \begin{cases} 2\left[\frac{h_w}{h_D} - 1\right](\bar{r} - 1) + \frac{h_w}{h_D} & \text{for } .5 \le r \le 1.0 \\ 1 + \frac{1}{2h_D}(u_D{}^2 - u_*{}^2) & \text{for } 0 \le r \le .5 \end{cases} \qquad (44)$$

where $u_* = u_D u^{(o)}$, the dimensional velocity; thus

$$f'(\bar{r}) = \begin{cases} 2\left[\frac{h_w}{h_D} - 1\right] & \text{for } .5 \le r \le 1.0 \\ -512\bar{r}^3(1-\bar{r})^3(1-2\bar{r})\frac{u_D{}^2}{h_D} & 0 \le r \le .5 \end{cases} \qquad (45)$$

and

$$f''(\bar{r}) = \begin{cases} 0 & \text{for } .5 \le r \le 1.0 \\ -512\bar{r}^2(1-\bar{r})^2(3 - 14\bar{r} + 14\bar{r}^2)\frac{u_D{}^2}{h_D} \end{cases} \qquad (46)$$

The Galerkin equations then reduce to:

$$\begin{cases} a_{11}A_1 + a_{12}A_2 = R_1 \\ a_{11}B_1 + a_{12}B_2 = R_2 \end{cases} \tag{47}$$

where A_1, A_2, B_1, B_2, R_1 and R_2 are given in Appendix II.
Solving for a_{11} and a_{12},

$$a_{11} = \frac{R_1\left(\frac{B_2}{A_1}\right) - R_2\left(\frac{A_2}{A_1}\right)}{B_2 - B_1\left(\frac{A_2}{A_1}\right)}$$

$$a_{12} = \frac{R_2 - R_1\left(\frac{B_1}{A_1}\right)}{B_2 - B_1\left(\frac{A_2}{A_1}\right)} \tag{48}$$

and it is noted that R_1 and R_2 depend on h_w/h_D and $u_D{}^2/h_D$.
Now, in dimensional terms,

$$\frac{1}{r}\frac{\partial h_{*1}^{(2)}}{\partial \theta} = \frac{h_D}{R}\frac{1}{\bar{r}}\frac{\partial h_1^{(2)}}{\partial \theta} = \frac{-h_D}{\beta^2 R}\left(\frac{2\theta}{\bar{r}}\right)\left\{a_{11} + a_{12}\beta^2\left(\frac{2\theta^2}{\beta^2} - 1\right)\right\}\sin\pi\bar{r}$$

which, at $\bar{r} = 1/2$ and $\theta = \beta$,

$$= -\frac{4h_D}{\beta R}\left\{a_{11} + 2\beta^2 a_{12}\right\} \tag{49}$$

VI. Free Shear Layer Solution of the Energy Equation

We assume that the enthalpy profile is "locally similar" and can be approximated in the matching plane by the Busemann Integral solution[14] (assuming a constant pressure free shear layer with Pr = 1.0): i.e., $H = Au + B$, with the boundary conditions:

$$\text{(i)} \quad H(u_3) = H_3$$
$$\text{(ii)} \quad H(u_D) = H_D \tag{50}$$

Thus,
$$A = \frac{H_3 - H_D}{u_3 - u_D}$$

and

$$\frac{\partial h}{\partial y} = \frac{\partial u}{\partial y}(A - u)$$

using the profile of Eq. (23)

$$\left.\frac{\partial h}{\partial y}\right|_{D^+} \cong \frac{H_3}{\delta_3}\left[(\overset{*}{u} - 1)^2 - \tilde{h}_D{}^+\right] \tag{51}$$

where the approximation $H_3 \simeq u_3{}^2/2$ has been used and the definitions made:

$$\tilde{h}_D{}^+ = h_D{}^+/H_3, \quad \overset{*}{u} = u_D/u_3 \tag{52}$$

VII. Matching Conditions

The matching conditions at $\bar{r} = 1/2$, $\theta = \beta$ are simply:

$$\begin{aligned} &\text{(i)} \quad \left[h_D\right]_-^+ = 0 \\ &\text{(ii)} \quad \left[q_D\right]_-^+ = 0 \end{aligned} \tag{53}$$

Thus, the enthalpy gradient is continuous and we obtain:

$$-\frac{4h_D}{\beta R}\left\{a_{11} + 2\beta^2 a_{12}\right\} = \frac{H_3}{\delta_3}\left[(\overset{*}{u} - 1)^2 - \tilde{h}_D\right]$$

or,

$$(\overset{*}{u} - 1)^2 - \tilde{h}_D + \frac{4}{\beta}\left(\frac{\delta_3}{R}\right)\left(\frac{\tilde{h}_D}{B_2 - B_1\left(\frac{A_2}{A_1}\right)}\right)\left\{R_1\left(\frac{B_2}{A_1}\right) - R_2\left(\frac{A_2}{A_1}\right) + 2\beta^2\left[R_2 - R_1\left(\frac{B_1}{A_1}\right)\right]\right\} = 0 \tag{54}$$

To solve for $\tilde{h}_D$, we must write I_6 and I_7 (integrals which appear in Eq. (42); see Appendix II) in the form:

$$I_6 = 2\left(\frac{\tilde{h}_w}{\tilde{h}_D} - 1\right)Q_1 - 1024Q_2\,\frac{\overset{*2}{u}}{\tilde{h}_D}$$

$$I_7 = \frac{2}{\pi}\left(\frac{\tilde{h}_w}{\tilde{h}_D} - 1\right) - .46\,\frac{\overset{*2}{u}}{\tilde{h}_D}$$

and define $\tilde{h}_w = \frac{h_w}{H_3}$

Now defining

$$\begin{cases} 32Q_1 Pe'(a_o I_9 - I_8) - \frac{2}{\pi} I_8 = N_1 \\ 32Q_1 Pe'(a_o I_{10} - I_{11}) - \frac{2}{\pi} I_{11} = N_2 \end{cases}$$

$$\begin{cases} 1.64 \times 10^4 Q_2(a_o I_9 - I_8) - .46 I_8 = M_1 \\ 1.64 \times 10^4 Q_2(a_o I_{10} - I_{11}) - .46 I_{11} = M_2 \end{cases}$$

we may solve for $\tilde{h}_D$

$$\tilde{h}_{D_1}^{(2)} = \frac{(\overset{*}{u}-1)^2 + \frac{4}{\beta}\left(\frac{\delta_3}{R}\right)\left\{\frac{\left(\frac{B_2 - 2\beta^2 B_1}{A_1}\right)\left(N_1 h_w - N_2 \overset{*2}{u}\right) - \left(\frac{A_2}{A_1} - 2\beta^2\right)\left(M_1 \tilde{h}_w - M_2 \overset{*2}{u}\right)}{B_2 - B_1(A_2/A_1)}\right\}}{1 + \frac{4}{\beta}\left(\frac{\delta_3}{R}\right)\left\{\frac{\left(\frac{B_2 - 2\beta^2 B_1}{A_1}\right) N_1 - \left(\frac{A_2}{A_1} - 2\beta^2\right) M_1}{B_2 - B_1(A_2/A_1)}\right\}} \qquad (55)$$

We may now calculate $\overset{*}{u}_1$ (subscripts now refer to the iteration-number) from Eq. (25) for a trial β. Inserting $\overset{*}{u}_1$ into the above, $\tilde{h}_{D_1}^{(2)}$ is known, and $\overset{*}{u}_2$ may be calculated from Eq. (27). A new trial β is selected until $\overset{*}{u}_2 \simeq \overset{*}{u}_1$, starting from $\beta = 1^o$ ($\overset{*}{u}_1$ decreases with β and $\overset{*}{u}_2$ increases with β; a convergent iteration results).

VIII. Busemann Integral Solution in the Recirculation Region

A still simpler approximate solution may be obtained by extending the free shear layer solution into the recirculation vortex, taking as a new boundary condition:

$$H = h_{core} \text{ at } u = 0$$

h_{core} is best approximated by assuming

$$h_{core} \approx h_{wall} \qquad (56)$$

(this assumption implies the absence of a thermal boundary layer on the base wall).

Then,
$$\frac{T_D}{T_3} = \frac{T_w}{T_3} + \left(1 - \frac{T_w}{T_3}\right)\overset{*}{u} + \left(\frac{\gamma-1}{2}\right)M_3^{\,2}\,\overset{*}{u}(1-\overset{*}{u}) \tag{57}$$

which replaces Eq. (55). Actually, the solution to Eqs. (25), (27) and (57) may be solved directly by assuming β, solving Eq. (27), with Eq. (57), for $\overset{*}{u}$ (a quadratic equation), and Eq. (25) for Re_{2S}. For the sake of uniformity of the program, however, T_D/T_3 was used in the iteration described. The results of this calculation will be discussed together with those of the previous section.

To relate the remaining unknowns to flight conditions, it is necessary to write down the inviscid flow field solutions. Given the velocity and altitude, ambient conditions are known and post-shock conditions are computed as follows:

$$M_1 = u_1/a_1, \quad Re_{1S} = \frac{\rho_1 u_1 S}{\mu_1} \tag{58}$$

Shock angle, δ, is obtained from

$$M_1^{\,2}\sin^2\delta - 1 = \left(\frac{\gamma+1}{2}\right) M_1^{\,2}\,\frac{\sin\delta\,\sin\alpha}{\cos(\delta-\alpha)} \tag{59}$$

Then,

$$M_2^{\,2} = \left[\frac{1}{\sin^2(\delta-\alpha)}\right]\left[\frac{1 + \frac{\gamma-1}{2}M_1^{\,2}\sin^2\delta}{\gamma M_1^{\,2}\sin^2\delta - \left(\frac{\gamma-1}{2}\right)}\right] \tag{60}$$

and with $M_{1_n} = M_1\sin\delta$, standard tables are used to compute p_2, ρ_2, T_2, a_2 and u_2. We assume the viscosity law $\mu_2/\mu_1 = (T_2/T_1)^{.76}$. The Prandtl-Meyer Function determines M_H (required for calculation of P_H) and M_3 from an expansion of α and $\alpha+\beta$ degrees, respectively. Isentropic equations give

$$\frac{T_3}{T_2} = \frac{1 + \frac{\gamma-1}{2}M_2^{\,2}}{1 + \frac{\gamma-1}{2}M_3^{\,2}} = \left(\frac{a_3}{a_2}\right)^2$$
$$\frac{P_{t_2}}{P_3} = \left[1 + \frac{\gamma-1}{2}M_3^{\,2}\right]^{\gamma/\gamma-1} \tag{61}$$

From the integral solution mentioned previously,[13]

$$\frac{\delta_2}{S} = \left[\frac{2(T_w/T_2)^{.76}}{(\theta/\delta)_2 \; Re_{2S}}\right]^{1/2} \tag{62}$$

where

$$Re_{2S} = \frac{\rho_2 u_2 S}{\mu_2} \tag{63}$$

$$\left(\frac{\theta}{\delta}\right)_2 = \frac{1}{m_2}\left[1 + \ell n \sqrt{1+m_2} - \sqrt{\frac{1+m_2}{m_2}}\,\ell n\,(\sqrt{1+m_2} + \sqrt{m_2})\right]$$

$$m_2 = \left(\frac{\gamma-1}{2}\right) M_2^{\,2}$$

The characteristic Reynolds number for the recirculation regions is

$$Re_B = \frac{\rho_3 u_D R}{\mu_w}$$

where (64)

$$R = S\left(\frac{\sin\alpha}{\sin\beta}\right)$$

Of course, T_w, α and S are given data and together with u_1 and altitude constitute the independent variables in this analysis.

IX. Numerical Results

Calculations have been carried out for the conditions of the wind-tunnel wedge experiment of Dewey[20]; $M_1 = 6$, $\alpha = 15^\circ$, $S = .0483$ ft and $T_o = 300^\circ F$. The base pressure was calculated over the Reynolds number range of the experiment for various values of η, the only free parameter in the solution. The theoretical base pressure decreases with η, due to the reduction of the dividing streamline stagnation pressure (Eq. (27)). Two results are shown in Fig. 5, from which it is apparent that a constant value of η yields a reasonable approximation to the data. The value $\eta = 0.6$ was selected based on the theoretical work of Reeves[15] (for $Re_{2H,\,NECK} = 3720$). It is seen, however, that $\eta = .4$ results in a theoretical curve that is never more than 20% from the data. This would indicate that the recompression

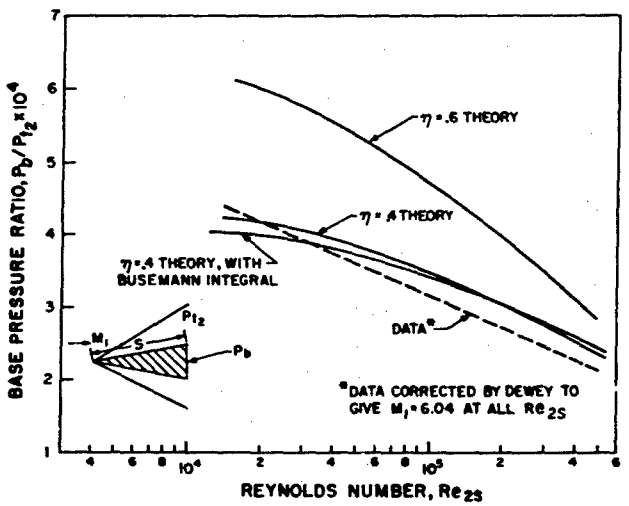

Fig. 5 Base pressure for a 15° half-angle wedge: from Dewey[20]

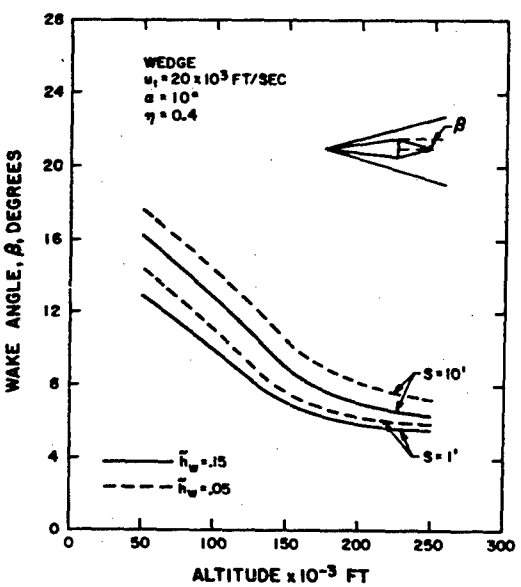

Fig. 6 Wake Angle of a Wedge vs Altitude

A2634
A2635

process is rather gradual, with the neck displaced significantly downstream of the DSL stagnation point. Additional calculations were carried out using a Busemann Integral approximation, Eq. (57). It is seen that some variation from the more exact solution occurs, due to the core temperature being held fixed at the wall temperature. To more precisely fix the stagnation enthalpy and to carefully investigate the effect of variable wall temperature, the Galerkin solution to the recirculation region enthalpy field is a necessary complication.

A series of calculations was performed to provide a rough understanding of the full-scale behavior of the near wake. Four representative wedges are considered: S = 1 ft and 10 ft and h_w = .05, .15 (typical of low temperature and high temperature ablators). The wake-angle, base pressure and stagnation enthalpy were calculated at various free-stream velocities and altitudes. These results are plotted in Figs. 6-8. In general, stagnation enthalpies decrease significantly with increasing altitude. The DSL velocity ratio, u^*, always decreases with increasing altitude, while h_D slowly increases and then decreases (at approximately 200,000 ft for u_1 = 20,000 ft/sec). The latter effect is due to the competition between thermal conduction and convection and the variation of the stagnation enthalpy: at the lower altitudes, the stagnation region is hot, but convection keeps the dividing streamline enthalpy down. As the altitude is increased, conduction begins to become dominant and increases h_D slightly. However, at still higher altitudes, the conversion of kinetic to thermal energy during recompression is markedly reduced and enthalpies everywhere begin to drop.

The effect of increasing wall temperature is qualitatively as expected. Significantly, it is seen in Fig. 8 that stagnation enthalpies of "cold" ten-foot bodies and "hot" one-foot bodies are comparable. At equal wall temperatures, however, the larger body has a stagnation enthalpy that is typically 25% higher. Furthermore, the calculated base pressures are 50% higher with a relatively hot wall, which qualitatively checks the experimental observations of Kurzweg.[21]

From Fig. 6, we observe that the near wake "dimensions" scale roughly as the body size for low and intermediate altitudes. At the higher

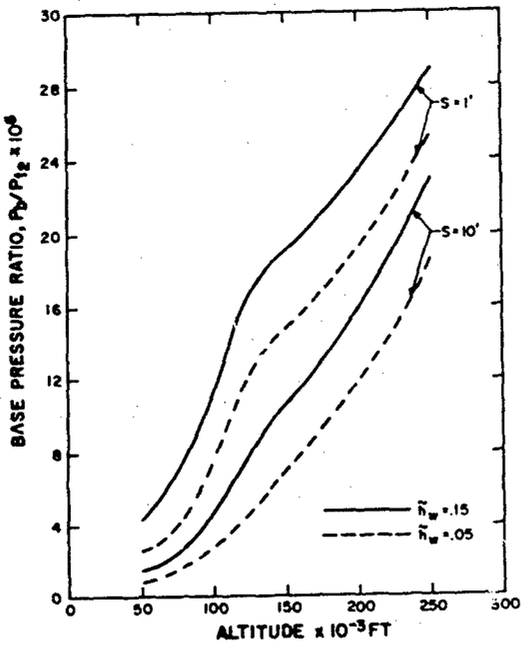

Fig. 7 Base Pressure Ratio for a Wedge vs Altitude

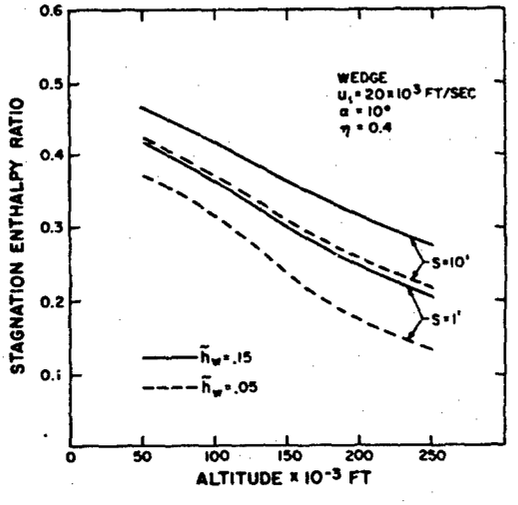

Fig. 8 Stagnation Enthalpy of a Wedge vs Altitude

A2636

A2637

altitudes, a small body exhibits a proportionately larger base region, but this never approaches the size of the near wake of the body used for comparison (additional calculations show that the wake angle increases slowly with increasing wedge angle).

The effect of free-stream velocity is exhibited in Fig. 9. Apparently, beyond 10,000 ft/sec there is very little influence of this parameter on the stagnation enthalpy ratio. At velocities below this, the greatest effects occur at high altitudes, indicating the small influence of variable velocity during a ballistic trajectory (assuming these results to be qualitatively correct for a three-dimensional body). Similar remarks apply to the wake angle and base pressure plotted in Figs. 6 and 7.

The effect of changing the only free parameter, η, is demonstrated to be small in Fig. 10. Because of the improved agreement with the experimental base pressures at $\eta = .4$, this value was assumed in the above calculations.

It was also found that the approximation solved, $h_1^{(2)}$, was sufficiently general to allow a boundary layer to develop along the dividing streamline. Enthalpy profiles at two altitudes are shown in Fig. 11, where the perturbation from the boundary value is seen to be only a few percent. It would be possible, of course, to accurately calculate the wall boundary layer with more terms in the radial direction. From the present computation, only a rough estimate of the base heat transfer can be obtained:

$$\frac{\partial h_{1_*}^{(2)}}{\partial r} = \frac{h_D}{R}\left[f'(\bar{r}) + (1 - \theta^2/\beta^2)\,(a_{11} + a_{12}\theta^2)\pi\cos\pi\bar{r}\right]$$

and, since

$$Q_b^* \equiv -k\left.\frac{\partial h_*}{\partial r}\right|_{\bar{r}=1}, \text{ the stagnation rate is}$$

$$Q_{b_1}^{*\,(2)}(0) = -\frac{kh_D}{R}\left[2\left(\frac{\tilde{h}_w}{\tilde{h}_D} - 1\right) - a_{11}\pi\right]$$

where $Q_b^* > 0$ implies heat transfer to the base. The variation of $Q^*(0)/\frac{kh_D}{R}$ with altitude is shown in Fig. 12, where it is always seen to be positive for cold wall conditions ($h_w = .05$) and negative for a relatively hot wall ($h_w = .15$).

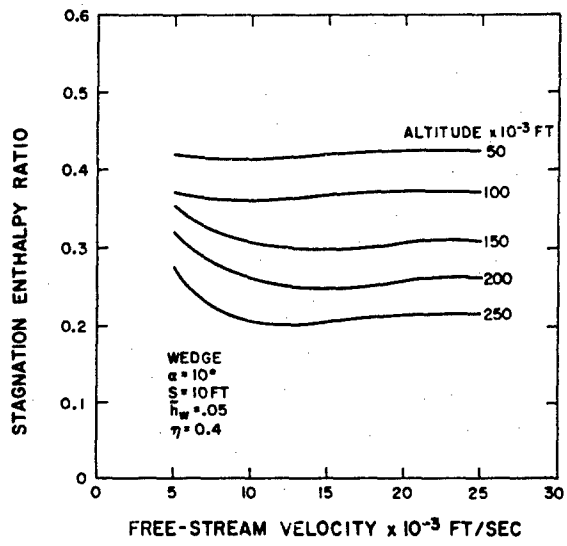

Fig. 9 Stagnation Enthalpy vs Free Stream Velocity at Various Altitudes

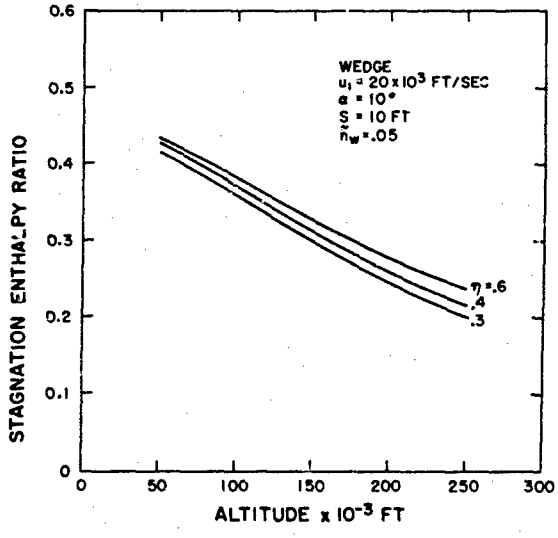

Fig. 10 Effect of η-parameter on Stagnation Enthalpy at Various Altitudes

A2638
A2639

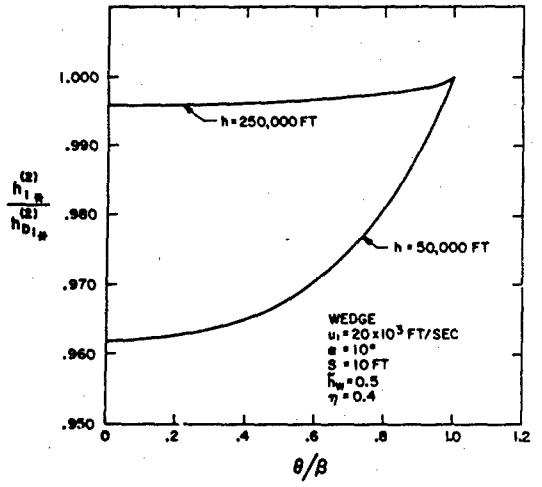

Fig. 11 Static Enthalpy Profiles at r = .5, Normalized to h_{D_*}

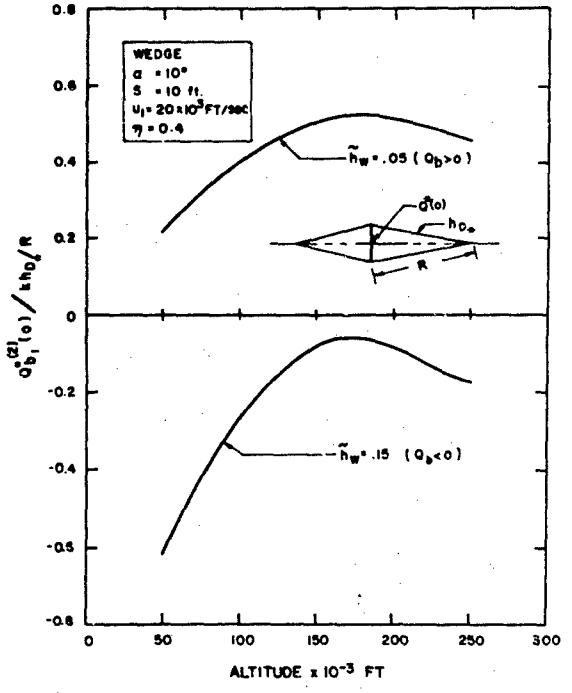

Fig. 12 Heat Transfer Rate at Base Wall Stagnation Point, Normalized vs Altitude

A2640
A2641

X. Summary and Extensions

A tractable and physically correct model of the two-dimensional near wake has been analyzed. The flow field was divided into subregions, including the recirculation regions, which were matched along mutual boundaries. The zeroth order solution of the velocity field was obtained from a series expansion of the streamfunction in local Reynolds number. Calculation of the uncoupled enthalpy field was carried out with a Galerkin procedure, with these results valid for arbitrary Reynolds number. Numerical results were obtained for the conditions of a wind-tunnel wedge experiment, and agreement of the base pressure variation with Reynolds number was satisfactory. Previous theories,[3, 4] it should be noted, have yielded results which are Reynolds number-independent. The effect of body size, wall temperature and free-stream velocity and density on the dividing streamline stagnation enthalpy was also investigated. It was found that the stagnation enthalpy ratio increased with decreasing altitude but was rather insensitive to Mach number at hypersonic speeds. An increase in wall temperature was found to significantly increase the stagnation enthalpy and base pressure. It was seen from calculations for two bodies, that near wake size scales directly with body size. Finally, it was shown that the stagnation enthalpy was relatively insensitive to changes in the ratio of dividing streamline stagnation pressure to neck pressure, the single free parameter in the solution. While simple improvements are possible in the two-dimensional analysis (solution of the free shear layer, multiple-point matching with the recirculation regions, etc.), it is anticipated that three-dimensional effects will be more important. The concentration of streamlines in the stagnation region, growth of the free shear layer displacement thickness (due to geometry alone), and the incompletely understood recompression process external to the dividing streamline are expected to make quantitative changes in the near wake solution. While the results presented herein are expected to indicate the general behavior of axisymmetric near wake properties, it must be emphasized that they (and all other presently available theories) are strictly applicable to two-dimensional flow fields.

ACKNOWLEDGMENT

The author is pleased to acknowledge the guidance and encouragement of Dr. Arnold Goldburg of Avco-Everett Research Laboratory, at whose suggestion this work was initiated. He is also indebted to Professor George Carrier and Dr. Sheldon Weinbaum for many helpful discussions.

APPENDIX I.

Expansion of the Boundary Layer

The geometry of this problem is shown below

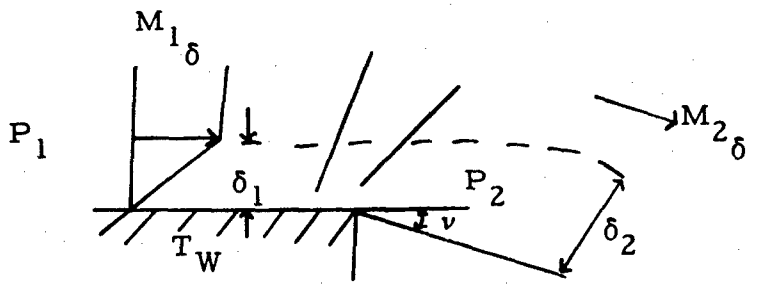

The assumptions are as follows:

(i) the rapid expansion process along streamlines is essentially isentropic

(ii) each streamline reaches the pressure P_2, as determined by turning the inviscid flow through the angle ν

(iii) the initial velocity profile is linear and the enthalpy profile is "similar" ($H_1 = Au_1 + B$)

(iv) $\gamma = 1.4$

The calculation procedure is simply to expand each streamline with P_o and T_o held constant, and calculate the velocity and density after expansion. We then conserve mass between streamlines to locate them after expansion, and to estimate the expanded boundary layer thickness. Denoting streamlines by i and conditions before and after expansion by 1 and 2, respectively, we can write

$$\frac{y_{2_{i+1}}}{\delta_1} = \frac{y_{2_i}}{\delta_1} + \frac{I_i}{n}$$

where $i = 0, 1, 2, \ldots . n$ and $y_{2_o} = 0$

$$I_i \equiv \frac{\left(\frac{\rho_{1_i}}{\rho_{1_\delta}}\right)\left(\frac{u_{1_i}}{u_{1_\delta}}\right) + \left(\frac{\rho_{1_{i+1}}}{\rho_{1_\delta}}\right)\left(\frac{u_{1_{i+1}}}{u_{1_\delta}}\right)}{\left(\frac{\rho_{2_i}}{\rho_{1_\delta}}\right)\left(\frac{u_{2_i}}{u_{1_\delta}}\right) + \left(\frac{\rho_{2_{i+1}}}{\rho_{1_\delta}}\right)\left(\frac{u_{2_{i+1}}}{u_{1_\delta}}\right)}$$

from "averaged" conservation of mass.

Also,

$$\frac{\rho_{1_i}}{\rho_{1_\delta}} = \frac{T_{1_\delta}}{T_{1_i}} \qquad \text{(equation of state)}$$

$$\frac{u_{1_i}}{u_{1_\delta}} = \frac{y_{1_i}}{\delta_1} \qquad \text{(given profile)}$$

and it can be shown that

$$\frac{\rho_{2_i}}{\rho_{1_\delta}} = \left(\frac{P_2}{P_1}\right)\left(\frac{P_{oi}}{P_2}\right)^{\frac{\gamma-1}{\gamma}} \left(\frac{T_{1_\delta}}{T_{o_\delta}}\right)\left(\frac{T_{o_\delta}}{T_{o_i}}\right)$$

$$\frac{u_{2_i}}{u_{1_\delta}} = \left(\frac{M_{2_i}}{M_{1_\delta}}\right)\left(\frac{T_{o_\delta}}{T_{1_\delta}}\right)^{1/2} \left(\frac{P_{oi}}{P_2}\right)^{-\left(\frac{\gamma-1}{2\gamma}\right)} \left(\left[1 - \frac{T_w}{T_{o_\delta}}\right]\frac{y_{1_i}}{\delta_1} + \frac{T_w}{T_{o_\delta}}\right)^{1/2}$$

$$M_{2_i} = \left(\frac{2}{\gamma-1}\right)^{1/2}\left[\left(\frac{P_{oi}}{P_2}\right)^{\frac{\gamma-1}{\gamma}} - 1\right]^{1/2}$$

$$\frac{T_{o_\delta}}{T_{1_\delta}} = 1 + \frac{\gamma-1}{2} M_{1_\delta}^{\ 2}$$

$$\frac{P_{oi}}{P_2} = \left(\frac{y_{1_i}}{\delta_1}\right)\left(\frac{T_{1_\delta}}{T_{1_i}}\right)^{1/2} M_{1_\delta}$$

$$\frac{T_{l_i}}{T_{l_\delta}} = \left(\frac{T_{o_i}}{T_{o_\delta}}\right)\left(\frac{T_{o_\delta}}{T_{l_\delta}}\right) - \frac{u_{l_\delta}^2}{2C_p T_{l_\delta}}\left(\frac{y_{l_i}}{\delta_l}\right)^2$$

$$\frac{T_{o_i}}{T_{o_\delta}} = \left(1 - \frac{T_w}{T_{o_\delta}}\right)\frac{y_{l_i}}{\delta_l} + \frac{T_w}{T_{o_\delta}}$$

$$\frac{u_{l_\delta}^2}{2C_p T_{l_\delta}} = \frac{T_{o_\delta}}{T_{l_\delta}} - 1$$

$$\frac{P_l}{P_2} = \left[\frac{1 + \frac{\gamma-1}{2} M_{2_\delta}^2}{1 + \frac{\gamma-1}{2} M_{l_\delta}^2}\right]^{\frac{\gamma}{\gamma-1}}$$

M_{2_δ} is obtained from the Prandtl-Meyer Tables

For $M_{l_\delta} > 10$, we may use

$$\frac{P_l}{P_2} \cong \left[1 - \left(\frac{\gamma-1}{2}\right) M_{l_\delta}\, \nu\right]^{-\frac{2\gamma}{\gamma-1}}$$

and

$$\frac{M_{2_\delta}}{M_{l_\delta}} \cong \left(\frac{P_l}{P_2}\right)^{\frac{\gamma-1}{2\gamma}}$$

It should first be pointed out that under the given boundary conditions, the expanded flow will be non-parallel. We must therefore assume some process to turn the inner streamlines back to the direction given by ν. A "lip shock" or combination of expansions and shocks is probably necessary, and this complicated region is presently under study. The assumption of constant P_o along the wall is also an obvious inconsistency, and requires a finite velocity to exist there after expansion. However, since experiments by Hammit[19] indicate the reasonableness of this approximation away from the wall, we allow "slip velocities" to be calculated and interpret them as velocities at the edge of a high-shear sub-layer.[22] A typical profile is

shown in Fig. 13 and δ_2/δ_1 is plotted against all the independent variables, M_{1_δ}, T_w/T_{o_δ} and ν in Figs. 14-15. It is seen that a significant thickening can occur, and the results are certainly limited by boundary layer-shock wave interaction. The most rapid changes with angle occur at the higher Mach number and the most significant Mach number effects are at low Mach number. Increasing wall temperature has the effect of decreasing the thickening and at a temperature ratio of 0.8, the $M_{1_\delta} = 2$ boundary layer actually becomes thinner for small angles of expansion (this is actually observed in Hammit's Schlieren photographs). The sub-program detailed above is used in the near wake solution with the following changes in nomenclature

$$\delta_1 \rightarrow \delta_2$$

$$\delta_2 \rightarrow \delta_2'$$

$$\nu \rightarrow \alpha + \beta$$

$$M_{1_\delta} \rightarrow M_2$$

$$\frac{T_w}{T_{o_\delta}} \rightarrow \tilde{h}_w$$

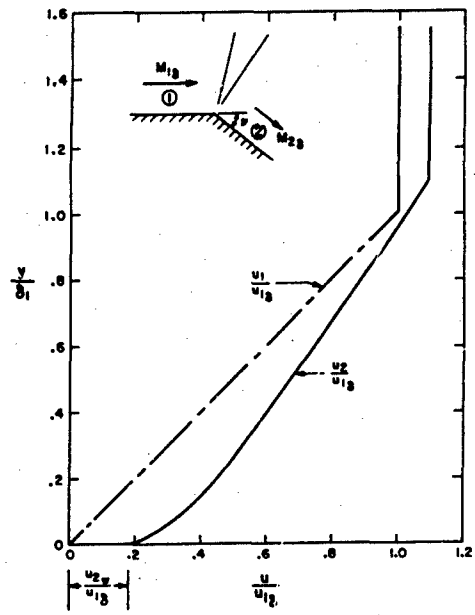

Fig. 13 Prandtl-Meyer Expansion of a Boundary Layer; Velocity Profile after Expansion at $M_{1_\delta} = 2.00$, $\nu = 10^o$, $T_w/T_{o_\delta} = 0.1$ ($\gamma = 1.4$)

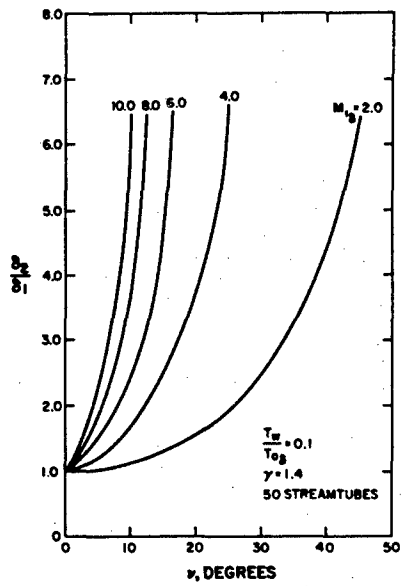

Fig. 14 Prandtl-Meyer Expansion of a Boundary Layer: δ_2/δ_1 vs. ν and M_{1_δ} for $T_w/T_{o_\delta} = 0.1$

A2642
A2643

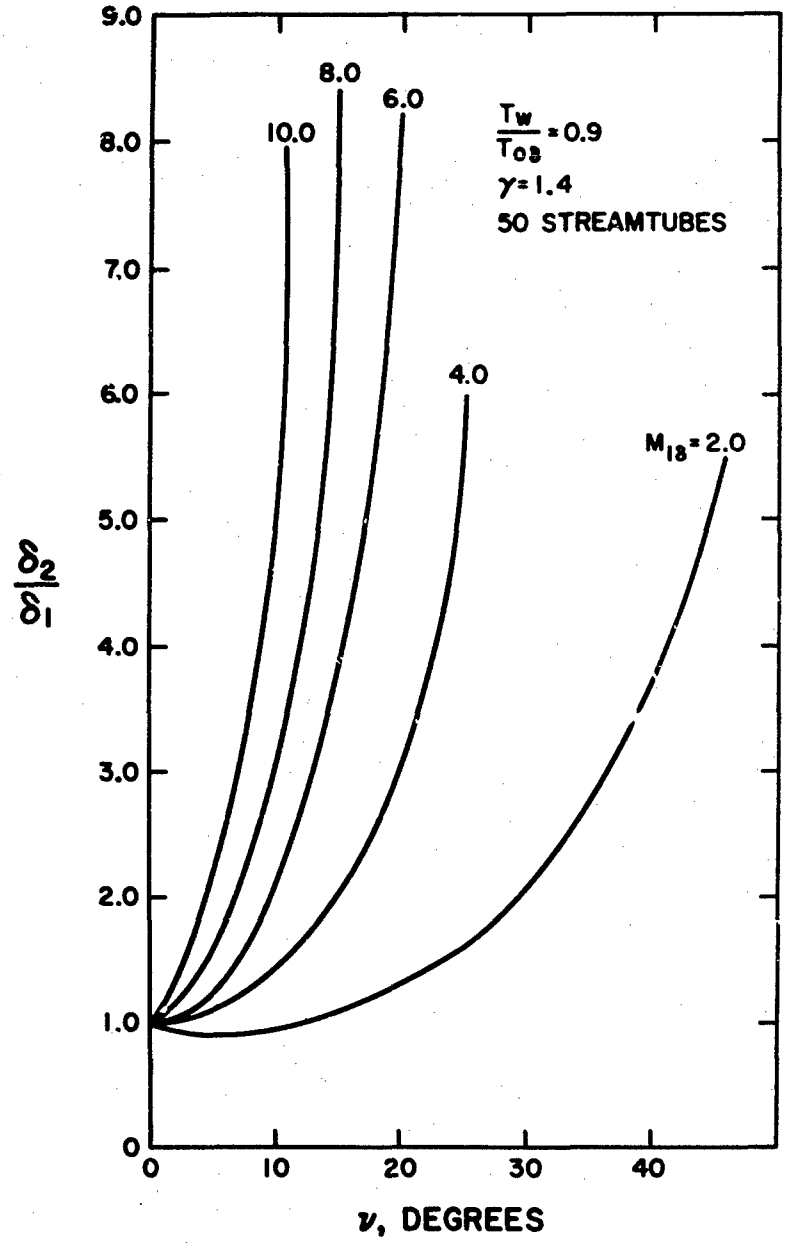

Fig. 15 Prandtl-Meyer Expansion of a Boundary Layer: δ_2/δ_1 vs. ν and M_{1_δ} for $T_w/T_{o_\delta} = 0.9$

APPENDIX II.

$$A_1 = -\pi^2 I_1 I_9 + \pi I_2 I_9 - \frac{2}{\beta^2} I_3 I_8 - 16P\acute{e}\pi I_4 \left[a_o I_{15} - I_9\right] - 32 \frac{mP\acute{e}}{\beta\Gamma} I_5 I_{13}$$

$$A_2 = -\pi^2 I_1 I_{10} + \pi I_2 I_{10} + 2 I_3 \left[I_8 - \frac{6}{\beta^2} I_{11}\right] - 16P\acute{e}\pi I_4 \left[a_o I_{12} - I_{10}\right] + 32 \frac{mP\acute{e}}{\Gamma} I_5 \left[I_{13} - \frac{2}{\beta^2} I_{14}\right]$$

$$R_1 = 16P\acute{e} I_6 \left[a_o I_9 - I_8\right] - I_7 I_8$$

$$B_1 = -\pi^2 I_1 I_{10} + \pi I_2 I_{10} - \frac{2}{\beta} I_3 I_{11} - 16P\acute{e}\pi I_4 \left[a_o I_{12} - I_{10}\right] - 32 \frac{mP\acute{e}}{\beta\Gamma} I_5 I_{14}$$

$$B_2 = -\pi^2 I_1 I_{16} + \pi I_2 I_{16} + 2 I_3 \left[I_{11} - \frac{6}{\beta^2} I_{19}\right] - 16P\acute{e}\pi I_4 \left[a_o I_{17} - I_{16}\right] + 32 \frac{mP\acute{e}}{\Gamma} I_5 \left[I_{14} - \frac{2}{\beta^2} I_{18}\right]$$

$$R_2 = 16P\acute{e} I_6 \left[a_o I_{10} - I_{11}\right] - I_7 I_{11}$$

$$I_1 = .25$$

$$I_2 = 0$$

$$I_3 = 1.22$$

$$I_4 = -2.09 \times 10^{-3}$$

$$I_5 = 1.32 \times 10^{-2}$$

$$Q_1 = 3.98 \times 10^{-2}$$

$$Q_2 = 1.16 \times 10^{-5}$$

$$I_8 = 2\beta/3$$

$$I_9 = 8\beta/15$$

$$I_{10} = 8\beta^3/105$$

$$I_{11} = 2\beta^3/15$$

$$I_{12} = 16\beta^3/315$$

$$I_{13} = \beta^3/20$$

$$I_{14} = 13\beta^5/840$$

$$I_{15} = 16\beta/35$$

$$I_{16} = 8\beta^5/315$$

$$I_{17} = 48\beta^5/3465$$

$$I_{18} = 34\beta^7/5040$$

$$I_{19} = 2\beta^5/35$$

$$a_o = 1.43$$

$$Pe' = \overset{*}{u}Pr\left(\frac{\rho_B u_3 S}{\mu_w}\right)\left(\frac{\sin\alpha}{\sin\hat{\beta}}\right)$$

$$Pr = 1.0$$

$$m = \frac{12}{\beta^3}\left(\frac{1}{a^2+b^2}\right)^2 [\sin(b\beta)\cosh(a\beta)(a^2-b^2+2ab) + \cos(b\beta)\sinh(a\beta)(a^2-b^2-2ab)]$$

$$-\frac{12}{\beta^2}\left(\frac{1}{a^2+b^2}\right) [\sin(b\beta)\sinh(a\beta)(a-bz) - \cos(b\beta)\cosh(a\beta)(b+az)]$$

REFERENCES

1. Lees, L., "Hypersonic Wakes and Trails," AIAA J., 2, 417-427 (March 1964).

2. Fromm, J., "A Method for Computing Nonsteady, Incompressible Viscous Fluid Flows," Los Alamos Scientific Laboratory LA-2910 (September 1963).

3. Chapman, D.R., "Laminar Mixing of a Compressible Fluid," NACA TN 1800 (1950).

4. Denison, M.R. and Baum, E., "Compressible Free Shear Layer with Finite Initial Thickness," AIAA J., 1, 342-349 (February 1963).

5. Goldstein, S., "Concerning Some Solutions of the Boundary Layer Equations in Hydrodynamics," Proc. Camb. Phil. Soc., 26, 1-30 (1930).

6. Viviand, H. and Berger, S., "The Incompressible Laminar Axisymmetric Wake Behind a Very Slender Cylinder in Axial Flow," Rept. No. AS-64-5, Inst. of Eng. Res., Univ. of Calif. (February 1964).

7. Kubota, T. and Dewey, C.F., "Momentum Integral Methods for the Laminar Free Shear Layer," AIAA J., 2, 625-629 (April 1964).

8. Ting, L. and Bloom, M.H., "On Stokes Flow in a Cavity," General Applied Science Laboratories TR 132 (December 1959).

9. Weinbaum, S.,"Criteria for a Flow to be Kinematically Similar to a Stokes Flow," to be published as an Avco-Everett Research Laboratory Research Report.

10. John, F., "Partial Differential Equations," New York Univ., Courant Inst. of Math.; Handbook of Physics, ed. by E. Condon and H. Odishaw, pp 1-75, McGraw-Hill, New York (1958).

11. Chandrasekhar, S. and Elbert, D., "On Orthogonal Functions which Satisfy Four Boundary Conditions. III. Tables for Use in Fourier-Bessel-type Expansions," Astrophys. J., Supp. Ser. 3, 453-458 (1958).

12. Kantorovich, L. and Krylov, V., Approximate Methods of Higher Analysis. P. Noordhoff Ltd., Netherlands, pp 253-269 (1958).

13. Truitt, R., Hypersonic Aerodynamics, p. 280. The Ronald Press Company, New York (1959).

14. Schlichting, H., Boundary Layer Theory, p. 341. McGraw-Hill, New York (1960).

15. Reeves, B., (Grad. Aeronaut. Lab., Calif. Inst. Tech.). Unpublished.

16. Whitham, G. B., Laminar Boundary Layers, ed. by L. Rosenhead, Oxford Univ. Press, pp. 124-127 (1963).

17. Charwat, A. and Yakura, J., "An Investigation of Two-dimensional Supersonic Base Pressures," J. Aeronaut. Sci., 25, 122 - 128 (February 1958).

18. Weinbaum, S., "Natural Convection Phenomena in Horizontal Circular Cylinders," Sperry Rand Research Center RR-63-14 (April 1963).

19. Murthy, K. and Hammit, A., "Investigation of the Interaction of a Turbulent Boundary Layer with Prandtl-Meyer Expansion Fans at M = 1.88," Princeton Univ. Rept. No. 434 (August 1958).

20. Dewey, C. F., "Measurements in Highly Dissipative Regions of Hypersonic Flows. Part II. The Near Wake of a Blunt Body at Hypersonic Speeds," Ph.D. Thesis, Calif. Inst. of Tech. (1963).

21. Kurzweg, H., "Interrelationship Between Boundary Layer and Base Pressure," J. Aeronaut. Sci., 18, 743-748 (November 1951).

22. Zakkay, V. and Tani, T., "Theoretical and Experimental Investigation of the Laminar Heat Transfer Downstream of a Sharp Corner," Polytech. Inst. of Brooklyn, PIBAL Rept. No. 708 (1961).

23. Batchelor, G., "A Proposal Concerning Laminar Wakes Behind Bluff Bodies at Large Reynolds Number," J. Fluid Mech., 1, 388-398 (1956).

DISTRIBUTION LIST for Contract No. AF 04(694)-414

Director, Advanced Research Projects Agency, Department of Defense, The Pentagon, 2B257, Washington 25, D.C.
Attn: Fred A. Keother (1 copy)
C. E. McLain (1 copy)
Mr. Hertzfeld (1 copy)

Defense Research Laboratories, General Motors Corporation, Santa Barbara, California - Attn: Cam Scharr (1 copy)

Headquarters Ballsitic Systems Division, Air Force Systems Command, Norton AFB, California - Attn: BSYDF (Lt. Jefferson) (2 copies)
BSTA (1 copy)

Air Force Cambridge Research Labs., Laurence G. Hanscom Field, Bedford, Massachusetts - Attn: Lew Block (1 copy)

Aerospace Corporation, Post Office Box 1308, San Bernardino, California - Attn: Paul Doherty (40 copies)

Systems Engineering Group (SEPIR), Wright-Patterson Air Force Base, Ohio 45433

Arnold Engineering Development Center, Arnold Air Force Station, Tennessee - Attn: AEYD (1 copy)
AES (1 copy)

MIT Lincoln Laboratories, Post Office Box 4188, San Bernardino, California - Attn: J. Vernon (1 copy)

U. S. Air Force Weapons Laboratory, Kirtland Air Force Base, Albuquerque, New Mexico - Attn: SWOIC (1 copy)
WLAX (1 copy)

Defense Documentation Center, Cameron Station, Alexandria, Virginia - (20 copies)

General Electric Company, Missile and Space Division, 3198 Chestnut Street, Philadelphia, Pennsylvania - Attn: J. Persh (1 copy)

General Electric Company, Valley Forge Space Technology Center, Space Sciences Laboratory, Post Office Box 8555, Philadelphia 1, Pa.
Attn: Lawrence I. Chasen, Manager
MSD Library (2 copies)

Headquarters U.S. Army Missile Command, Redstone Arsenal, Alabama - Attn: A. Jenkins (AMSMI-RRX) (1 copy)

Massachusetts Institute of Technology, Lincoln Laboratory, Post Office Box 73, Lexington 73, Massachusetts -
Attn: G.B. Pippert (1 copy)
Mary A. Granese,
Document Librarian (1 copy)
Dr. Ellen Bressel (1 copy)
Dr. Frank McNamara (1 copy)

University of Michigan, Institute of Sciences and Technology, Post Office Box 618, Ann Arbor, Michigan - Attn: Infrared Information and
Analysis Group (1 copy)
BAMIRAC Library (1 copy)
Richard Jamron (1 copy)

U. S. Atomic Energy Commission, Washington 25, D.C. - Attn: Headquarters Library (1 copy)

U. S. Atomic Energy Commission, Division of Technical Information Extension, Post Office Box 62, Oak Ridge, Tennessee - (1 copy)

Polytechnic Institute of Brooklyn Aero. Lab., 527 Atlantic Ave., Freeport, N.Y., 11520 (1 copy) New York - Attn: Prof. Martin Bloom
(1 copy)

Heliodyne Corporation, 2365 Westwood Boulevard, Los Angeles 64, California - Attn: Dr. Saul Feldman (1 copy)

Hughes Aircraft Company, Groud Systems Group, Fullerton, California - Attn: Library, Bldg. 600 (1 copy)

Hughes Aircraft Company, Florence and Teale, Culver City, California - Attn: Mr. Nicholas E. Devereau, Technical Document Center
(1 copy)

The Mitre Corporation, Post Office Box 208, Bedford, Massachusetts - Attn: Library (1 copy)

Plasmadyne Corporation, 3829 South Main Street, Santa Ana, California - Attn: Document Control (1 copy)

Aeronautical Research Associates of Princeton, Inc., 50 Washington Road, Princeton, New Jersey - Attn: Dr. Coleman deP. Donaldson (1 copy)

Sandia Corporation Livermore Laboratory, Post Office Box 969, Livermore, California - Attn: Technical Library (1 copy)

Stanford Research Institute, Menlo Park, California - Attn: Acquisitions (1 copy)

Bendix Corporation, Bendix Products Division, 3300 West Sample Street, South Bend, Indiana - Attn: M. Katz (1 copy)

Bendix Corporation, Bendix Systems Division, 3300 Plymouth Road, Ann Arbor, Michigan - Attn: Library (1 copy)

The Boeing Company, Aerospace Division, P.O. Box 3707, Seattle 24, Washington - Attn: Library Unit Chief (1 copy)

Chrysler Corporation, Missile Division, Post Office Box 2628, Detroit 31, Michigan - Attn: Technical Information Center (1 copy)

General Dynamics/Astronautics, Post Office Box 1128, San Diego 12, California - Attn: Library and Information Services (128-00) (1 copy)

Cornell Aeronautical Laboratory, 4455 Genesee Street, Buffalo, New York - Attn: Library (1 copy)

Defense Research Corporation, 4050 State Street, Santa Barbara, California - Attn: Technical Information Office (1 copy)

Douglas Aircraft Company, 3000 Ocean Park Boulevard, Santa Monica, California - Attn: Library (1 copy)

Electro-Optical Systems, Inc., 125 North Vinedo Avenue, Pasadena, California - Attn: Mr. M. Richard Dension, Head,
Aerospace Physics Dept.
Fluid Physics Division (1 copy)

Avco Corporation, Research and Advanced Development Division, 201 Lowell Street, Wilmington, Massachusetts - Attn: D. Walker (1 copy)
R. Detra (1 copy)
J. Luceri (1 copy)

Commander (Code 753) U.S. Naval Ordnance Test Station, China Lake, California - Attn: Technical Library (1 copy)

Space Technology Laboratories, Inc., One Space Park, Redondo Beach, California - Attn: L. Hromas (1 copy)

AUTIC, The Martin Company, Post Office Box 179, Denver, Colorado (1 copy)

McDonnell Aircraft Corporation, Lambert-Saint Louis Municipal Airport, Box 516, St. Louis 66, Missouri (1 copy)

Office of Aerospace Research, Tempo-D, Washington 25, D.C. - Attn: RROSE (1 copy)

Chief, AFSC Office, Room C-107, Bldg. 4488, Redstone Arsenal, Alabama (1 copy)

Lockheed Missiles and Space Company, 7701 Woodley Avenue, Van Nuys, California - Attn: Technical Information Center, Dept. 50-14 (1 copy)

U.S. Naval Ordnance Laboratory, White Oak, Silver Spring, Maryland - Attn: Dr. R.K. Lobb, Aeroballistics Program Chief (1 copy)
Librarian (1 copy)

Sandia Corporation, Sandia Base, Post Office Box 5800, Albuquerque, New Mexico - Attn: R.W. Henderson (1 copy)
Document Control (1 copy)
E.W. Draper (1 copy)

Department of the Navy, Special Projects Office, Washington 25, D.C. - Attn: Mr. M. Schindler (1 copy)

Director U.S. Naval Research Lab., Washington, D.C. - Attn: Code 2027 (1 copy)

Lockheed Missiles and Space Company, Post Office Box 504, Sunnyvale, California - Attn: Mr. Maurice Tucker (1 copy)

Martin Company, SCI-Technical Library, Mail 398, Aerodynamics Laboratory, Baltimore 3, Maryland (1 copy)

Commanding Officer, U.S. Army Research Office (Durham),Box CM Duke Station, Durham, North Carolina (1 copy)

Battelle Memorial Institute, 505 King Avenue, Columbus, Ohio - Attn: Battelle DEFENDER (1 copy)

Office, Chief of Research and Development, Department of the Army, Washington 25, D.C. (1 copy)

U.S. Army Electronic Research and Development Laboratory, Fort Monmouth, New Jersey - Attn: Technical Library (1 copy)

Director, Ames Research Center, National Aeronautics & Space Administration, Moffett Field, California - Attn: Technical (1 copy)

Rome Air Development Center, Griffiss AFB, New York - Attn: RCLS/J. Segal (1 copy)

Office of Naval Research, Department of the Navy, Washington, D.C. - Attn: Dr. Shirleigh Silverman, Science Director (1 copy)

The Rand Corporation, 1700 Main Street, Santa Monica, California - Attn: Helen J. Waldron, Librarian (1 copy)

National Aeronautics & Space Administration, Aeronautical Research, 1520 H Street, N.W., Washington 25, D.C.
Attn: Mr. Bertram A. Mulcahy, Director,
Technical Information Division (1 copy)

Johns Hopkins University, Applied Physics Laboratory, 8621 Georgia Avenue, Silver Spring, Maryland - Attn: Dr. Gibson, Director (1 copy)

Dr. Antonio Ferri, Dept. of Aeronautics and Astronautics, New York University, School of Engineering and Science, Bronx 53, New York (1 copy)

University of California, Lawrence Radiation Laboratory, Livermore, California - Attn: Document Control - C. G. Craig (1 copy)

Lewis Research Center, National Aeronautics and Space Administration, 21000 Brookpark Road, Cleveland 35, Ohio - Attn: George Mandel, Librarian (1 copy)

DASA Chief, Washington 25, D.C. (1 copy)

Chief, Bureau of Naval Weapons (RT), Department of the Navy, Washington 25, D.C. - Attn: Weapons Systems Analysis Division (1 copy)

Bell Telephone Laboratories, Inc., Whippany, New Jersey - Attn: Technical Reports Center, Room 2A165B (1 copy)

Institute of Defense Analyses, Research and Engineering Support Division, Washington, D.C. - Attn: Library (1 copy)

Langley Research Center, National Aeronautics and Space Administration, Langley Station, Hampton, Virginia - Attn: Jean B. Elliott, Librarian (1 copy)

Massachusetts Institute of Technology, Instrumentation Laboratory, 68 Albany Street, Cambridge 39, Massachusetts - Attn: Library, W1-109 (1 copy)

Cornell University, Nuclear Studies Laboratory, Ithaca, New York - Attn: Prof. Hans Bethe (1 copy)

Jet Propulsion Laboratory, California Institute of Technology, 4800 Oak Grove Drive, Pasadena, California - Attn: H. Denslow, Library Supervisor (1 copy)

Guggenheim Aeronautical Laboratory, California Institute of Technology, 1201 E. California, Pasadena 4, California
Attn: Dr. H.W. Liepmann (1 copy)

University of California, Los Alamos Scientific Laboratory, Post Office Box 1663, Los Alamos, New Mexico - Attn: Document Control (1 copy)

Bureau of Naval Weapons Representative, Lockheed Missiles and Space Company (Special Projects Office), P.O. Box 504, Sunnyvale, California (1 copy)

Commander, U.S. Naval Air Missile Test Center, Point Mugu, California (1 copy)

Philco Corporation, Aeronutronic Division, Ford Road, Newport Beach, California - Attn: Technical Library (1 copy)

Vidya, Inc., 2626 Hanover Street, Stanford Industrial Park, Palo Alto, California - Attn: Patricia L. Horn, Security Officer (1 copy)

Systems Engineering Group, Deputy for Systems Engineering, Directorate of Technical Publications and specifications (SEPRR), Wright-Patterson Air Force Base, Ohio 45433 (1 copy)

Headquarters, Aeronautical Systems Div., U.S.A.F., Wright-Patterson, AFB, Ohio - Attn: W. D. Dodd (ASRSMF) (1 copy)
ASQWR (Lt. Hill) (1 copy)
A.M. Prettyman (1 copy)